VOLUME LXXVII NUMBER 2

THE ASTROPHYSICAL JOURNAL

AN INTERNATIONAL REVIEW OF SPECTROSCOPY AND ASTRONOMICAL PHYSICS

Edited by

GEORGE E. HALE
Mount Wilson Observatory of the Carnegie Institution of Washington

EDWIN B. FROST
Yerkes Observatory of the University of Chicago

HENRY G. GALE
Ryerson Physical Laboratory of the University of Chicago

OTTO STRUVE
Yerkes Observatory of the University of Chicago

MARCH 1933

THE UNIVERSITY OF CHICAGO PRESS
CHICAGO, ILLINOIS, U.S.A.

March 1933 Vol. LXXVII, No. 2

THE ASTROPHYSICAL JOURNAL

AN INTERNATIONAL REVIEW OF SPECTROSCOPY AND ASTRONOMICAL PHYSICS

The Astrophysical Journal is published by the University of Chicago at the University of Chicago Press, 5750 Ellis Avenue, Chicago, Illinois, during each month except February and August. ¶ The subscription price is $6.00 a year; the price of single copies is 75 cents. Orders for service of less than a half-year will be charged at the single-copy rate. ¶ Postage is prepaid by the publishers on all orders from the United States, Mexico, Cuba, Porto Rico, Panama Canal Zone, Republic of Panama, Dominican Republic, Canary Islands, El Salvador, Argentina, Bolivia, Brazil, Colombia, Chile, Costa Rica, Ecuador, Guatemala, Honduras, Nicaragua, Peru, Hayti, Uruguay, Paraguay, Hawaiian Islands, Philippine Islands, Guam, Samoan Islands, Balearic Islands, Spain, and Venezuela. ¶ Postage is charged extra as follows: for Canada and Newfoundland, 30 cents on annual subscriptions (total $6.30); on single copies, 3 cents (total 78 cents); for all other countries in the Postal Union, 80 cents on annual subscriptions (total $6.80), on single copies, 8 cents (total 83 cents). ¶ Patrons are requested to make all remittances payable to The University of Chicago Press, in postal or express money orders or bank drafts.

The following are authorized agents:

For the British Empire, except North America, India, and Australasia: The Cambridge University Press, Fetter Lane, London, E.C. 4. Prices of yearly subscriptions and of single copies may be had on application.

For Japan: The Maruzen Company, Ltd., Tokyo.

For China: The Commercial Press, Ltd., 211 Honan Road, Shanghai. Yearly subscriptions, $6.00; single copies, 75 cents, or their equivalents in Chinese money. Postage extra, on yearly subscriptions 80 cents, on single copies 8 cents.

Claims for missing numbers should be made within the month following the regular month of publication. The publishers expect to supply missing numbers free only when losses have been sustained in transit, and when the reserve stock will permit.

Business correspondence should be addressed to The University of Chicago Press, Chicago, Illinois.

Communications for the editors and manuscripts should be addressed to: Otto Struve, Editor of THE ASTROPHYSICAL JOURNAL, Yerkes Observatory, Williams Bay, Wisconsin.

The cable address is "Observatory, Williamsbay, Wisconsin."

The articles in this journal are indexed in the *International Index to Periodicals*, New York, N.Y.

Applications for permission to quote from this journal should be addressed to The University of Chicago Press, and will be freely granted.

Entered as second-class matter, January 17, 1895, at the Post-Office, Chicago, Ill., under the act of March 3, 1879.
Acceptance for mailing at special rate of postage provided for in Section 1103, Act of October 3, 1917, authorized on July 15, 1918.

PRINTED IN THE U.S.A.

THE ASTROPHYSICAL JOURNAL

AN INTERNATIONAL REVIEW OF SPECTROSCOPY AND ASTRONOMICAL PHYSICS

VOLUME LXXVII MARCH 1933 NUMBER 2

A STUDY OF THE SPECTRUM VARIABLE 73 DRACONIS

By W. W. MORGAN

ABSTRACT

The A2 dwarf 73 Draconis is a spectrum variable of the α Canum Venaticorum type. The *Eu* II line λ 4205 varies in intensity in a period of 20.7 days. *Fe* II–*Ti* II 4549 and the *Ti* II lines λ 4501 and λ 4571 vary in phase with λ 4205. It is possible that a number of other lines also vary in intensity. Wave-lengths and identifications for 477 lines between the limits λ 3902 and λ 4958 are given. A discussion of the relative number of atoms in the different states of excitation by the method of Russell and Adams is given for *Fe* I and *Cr* I. The number of atoms in the higher states of *Fe* I is about the same for 73 Draconis and the "normal" A2 dwarf ϵ Serpentis, while there are twenty-five times as many atoms effective in absorbing low-level lines in the latter star as in the former. Two very peculiar features of the spectrum are the weakness of *Ca* II K and the presence of numerous lines of *Cr* I which are, except for the lines of very low excitation, actually stronger than in the sun. The lines of *Cr* II are also strong, and the spectrum can be considered as representative of the "chromium stars."

1. The spectrum of 73 Draconis is given as A2p by the *Henry Draper Catalogue*. The spectrum was considered peculiar because of the strength of the *Sr* II line λ 4077 and the *Si* II doublet λ 4128 and λ 4130. On Yerkes plates the violet component of the doublet is blended while the red component is very weak. There seems to be little doubt that, unless *Si* II is variable in intensity, the lines are faint in 73 Draconis. The line *Sr* II 4077 is of moderate intensity, while the other component of the ultimate doublet at λ 4215 is the strongest line in the spectrum with the exception of the Balmer series of hydrogen. The difference in the intensity of the two lines is marked.

A conspicuous feature of the spectrum is the presence of a large

number of lines due to *Fe* I, *Cr* I, and *Cr* II. Most of the lines of *Fe* I of temperature classes III, IV, and V which have an intensity of 3 or more on Rowland's scale in the sun are present in 73 Draconis. Almost all the *Cr* I lines of intensity 5 or greater on King's scale are present. All the *Cr* II lines in the region observed are present, both the ones observed in the laboratory and the predicted members. The singlets of *Mg* I are strong, and the *Mg* II line at λ 4481 is one of the strongest in the spectrum. To be consistent with the presence of numerous arc lines of iron and chromium, we should expect the *Ca* II line K to be strong, but on plates which extend sufficiently far into the violet to show this region of the spectrum, we find that *Ca* II K is no stronger than several iron arc lines in its vicinity. K is fainter than in normal A0 stars like Sirius and Vega, and is even weaker than in B9 and B8 stars, where all of the arc lines have disappeared.

In addition to these peculiarities there are several strong lines for which no adequate identification can be found. The strongest of these is at λ 4423.0. This is probably the same line which was found to be strong in several A-type spectra by Adams and Joy.[1] They identified the line with *Y* II. Yttrium contributes somewhat to the line, but the wave-length, which has been measured on several plates, shows that much of the strength cannot be accounted for by this element. The line is broader than an unblended line should be.

2. From an examination of several early plates of the star, the line at λ 4205, which is probably due to *Eu* II, was suspected of varying in intensity. The suspected variability was confirmed and an announcement made in this *Journal*.[2] The star was put on the observing program of the one-prism spectrograph and a series of plates obtained during the summer and autumn of 1932. The plates have a scale of 30 A per millimeter at λ 4500.

Figure 1*a* gives the intensities of λ 4205 plotted according to time. A period of $20\overset{d}{.}7$ was found which fitted the observations satisfactorily. An examination of the spectrograms showed that other lines vary in intensity, the most marked being *Fe* II–*Ti* II 4549. Its intensities are plotted in Figure 1 *b*. The phases of maxima and minima coincide with those of λ 4205, but the maxima are wider

[1] *Publications of the Astronomical Society of the Pacific*, **38**, 124, 1926.

[2] *Astrophysical Journal*, **76**, 275, 1932.

than the minima. The two other strongest *Ti* II lines in the vicinity, at λ 4501 and λ 4571, are also variable, but the amplitude is less than for λ 4205 and λ 4549. Mean curves of variation for all four lines are given in Figure 2. The ordinates are arbitrary scales of intensity; the

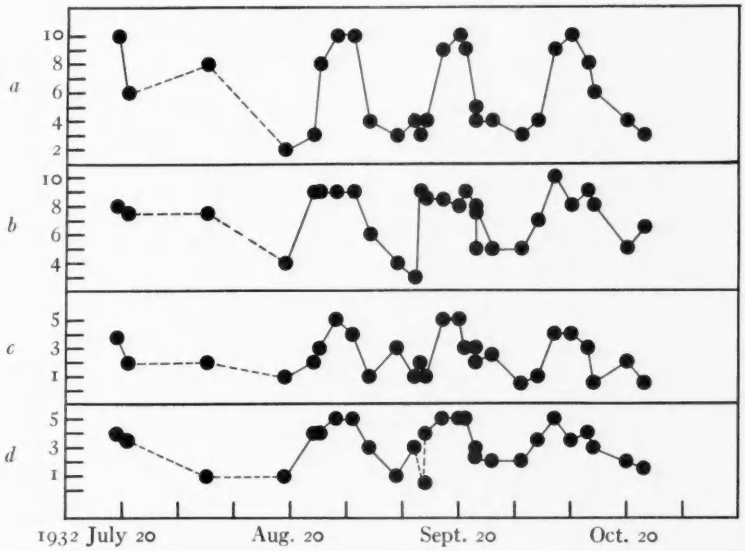

FIG. 1.—Variations in intensity of: (*a*) *Eu* II 4205, (*b*) *Fe* II–*Ti* II 4549, (*c*) *Ti* II 4501, and (*d*) *Ti* II 4571. Ordinates are units of intensity on an arbitrary scale; abscissae are expressed in ten-day units.

abscissae are tenths of the period. The elements of variation, counting from phase zero, are:

$$1932 \text{ July } 19.0+20^{d}7E \text{ (U.T.)}$$
$$\text{J.D. } 2426908.0+20^{d}7E \text{ (U.T.)}$$

The estimates of intensity are given in Table I.

From the fact that the two weaker *Ti* II lines vary in phase with *Fe* II–*Ti* II 4549, it seems probable that most, if not all, of the change in intensity of λ 4549 is due to the *Ti* II component of the blend. The other *Fe* II lines vary little if at all. The line at λ 4571 is a member of the same multiplet as *Ti* II 4549, and the curves of variation are quite similar. On the other hand, there is some evi-

dence that λ 4501, which is a member of a different multiplet, has a narrower maximum. It will be necessary to secure a better series of plates to investigate the other strong *Ti* II lines which are located

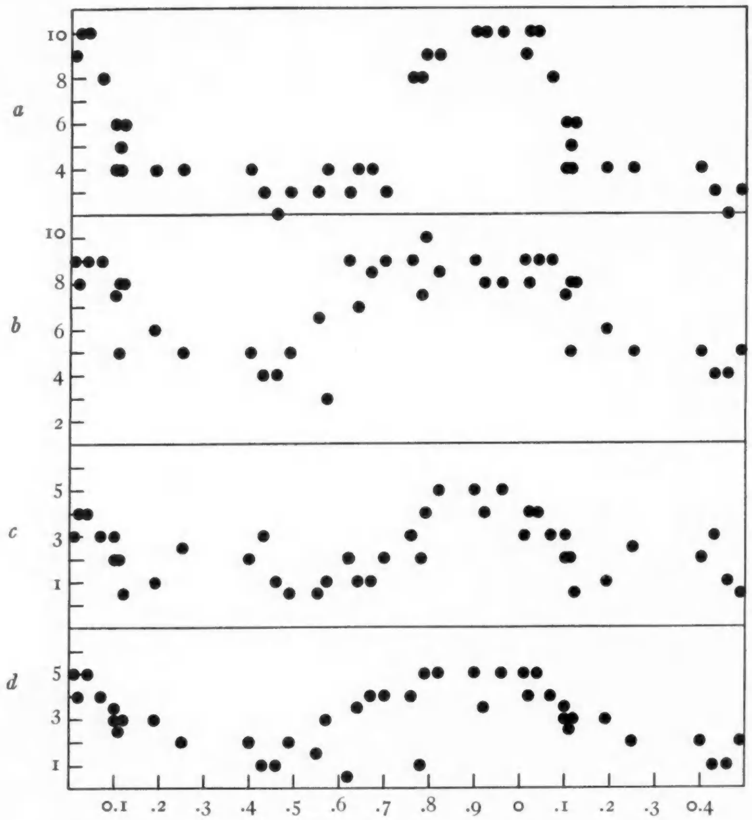

FIG. 2.—Mean curves of variation for: (*a*) *Eu* II 4205, (*b*) *Fe* II–*Ti* II 4549, (*c*) *Ti* II 4501, (*d*) *Ti* II 4571. Ordinates are intensity units on an arbitrary scale; abscissae are tenths of the period 20ᵈ7.

below *H*γ. More strongly exposed plates in the violet region will also be necessary for the investigation of the strong *Eu* II line at λ 4129. The unknown line at λ 4423.0 seems to vary in intensity, but there is no correlation with the twenty-day period found for λ 4205. It is possible, though not probable, that the variation is not real. It is also possible that a number of other lines vary in intensity, but, if

so, the amplitude is small and I believe it safer to leave the question of their variability open until better observational material is available.

TABLE I

ESTIMATED INTENSITIES OF VARIABLE LINES IN 73 DRACONIS

Date, 1932	Phase	*Eu* II 4205	*Ti* II–*Cr* I 4501	*Fe* II–*Ti* II 4549	*Ti* II–*Cr* II 4571
July 19.4	.02	10	4	8	4
21.1	.10	6	2	7.5	3.5
Aug. 4.2	.78	8	2	7.5	1
18.3	.46	2	1	4	1
23.3	.70	3	2	9	4
24.4	.76	8	3	9	4
27.3	.90	10	5	9	5
30.3	.04	10	4	9	5
Sept. 2.4	.19	4	1	6	3
7.4	.43	3	3	4	1
10.3	.57	4	1	3	3
11.3	.62	3	2	9	0.5
12.3	.67	4	1	8.5	4
15.3	.82	9	5	8.5	5
18.3	.96	10	5	8	5
19.3	.01	9	3	9	5
21.2	.10	4	3	7.5	3
21.3	.11	4:	2:	5:	2.5:
21.4	.11	5	2	8	2.5
24.3	.25	4	2.5	5	2
29.2	.49	3	0.5	5	2·
Oct. 2.3	.64	4	1	7	3.5
5.4	.79	9	4	10	5
8.2	.92	10	4	8	3.5:
11.3	.07	8	3	9	4
12.3	.12	6	0.5	8	3
18.1	.40	4:	2:	5	2
21.3	.55	3	0.5	6.5	1.5

The observers who participated in the taking of the plates were O. Struve, C. C. Crump, R. van Arnam, F. E. Roach, P. C. Keenan, H. F. Schwede, Miss C. Westgate, F. R. Sullivan, and W. W. Morgan.

With respect to the variability of the europium line, λ 4205, 73 Draconis is similar to α^2 Canum Venaticorum. The former is of a later spectral type than the latter, and the appearance of the spectrum is rather different. As far as finding a cause for the variation in intensity goes, we are as much in the dark as in the case of α^2 Canum Venaticorum. It is probable that when we find the cause of the variation of such stars we will also know why europium is so strong

in certain of the A-type stars. It would be of some interest to investigate the light of 73 Draconis photometrically for variation in the twenty-day period.

3. Although the star is fainter than can ordinarily be reached with Process plates, it was possible to obtain one plate on that fine-grain emulsion. All the lines visible on this plate were measured for wavelength. To check as far as possible, all lines were also measured on the best Eastman 40 plate. As the Process plate showed many more lines than those obtained on the coarser emulsion, the duplication was not complete. The wave-lengths and identifications are given in Table II. The columns are: the wave-length; the intensity on the Process plate; and the identification, intensity, and temperature class of the line as observed in the laboratory (King). Laboratory intensities other than King's are given in parentheses. Lines of *Fe* II which were not observed in the laboratory, but were predicted and picked out due to their behavior in the solar disk and spot spectra, are marked by asterisks in the intensity column.

THE ELEMENTS PRESENT

Probably the best way to bring out the departures from the normal strength of the elements at class A2 is to compare the spectrum, element by element, with a normal A2 dwarf. The spectrum of the star ϵ Serpentis has been investigated by Miss G. Farnsworth and the writer.[3] It is a good example of an average A2 dwarf. A description is given below of the behavior of the elements in the two stars.

H.—The lines of the Balmer series are of about the same intensity in the two stars. They are somewhat weaker than in Sirius.

Mg I.—The singlets are of about the same intensity in both stars. The unblended line at λ 4167 is of intensity 5 in 73 Draconis and 4 in ϵ Serpentis. As all the lines are slightly sharper in 73 Draconis than in ϵ Serpentis, the difference in intensity is less than the errors of observation and *Mg* I probably is identical in the two stars.

Mg II.—The doublet at λ 4481 is very strong in both stars. It is estimated to be of intensity 10 in both 73 Draconis and ϵ Serpentis. Possibly other fainter lines contribute to blends in both stars. The behavior of *Mg* II is identical.

[3] *Astrophysical Journal*, in press.

TABLE II

WAVE-LENGTHS AND IDENTIFICATIONS OF LINES

Star	Int.	Identification
3902.93	4	*Cr* I .88 12 II, *Fe* I .95 20 II
3903.98	4	*Fe* I .90 5 IV. (*Mg* I .96?)
3911.94	4	*Cr* I {.81, .98} 10 n III
3918.35	4	*Fe* I .32 (2), *Fe* I .42 3 IV, *Fe* I .65 4 IV
3919.24	3	*Cr* I .16 35 II
3920.72	a4n	*Fe* I .26 20 I, *Fe* I .85 (1), *Cr* I 1.02 20 I
3923.12	4N	*Fe* I 2.92 25 I
{3925.06, 3926.07}	{v, 4N, r}	*Fe* I 5.20 (1), *Fe* I 5.65 4 IV, *Fe* I 5.95 6 IV, *Fe* I 6.00 (1)
3926.72	2–3	*Cr* I .65 3 IV
3927.94	4–5	*Fe* I .93 30 I
3928.88	2	*Cr* I .64 25 I, *Fe* I 9.12 (1), *Fe* I 9.22 (1)
3930.35	2	*Fe* I .30 25 I, *Eu* II .50 300 III E
3932.73	2–3	*Fe* I .64 4 IV, *Fe* I .92 (1)
3933.64	6	*Fe* I .61 (2) IV, *Ca* II .66 400 II
3935.87	a5–6N	*Fe* I .82 8 III
3938.46	6	*Mg* I .43 (3r)
3939.12	2	*Fe* II (.15) (⊙)
3941.24	5n	*Fe* I 0.89 5 II, *Fe* I 1.29 (2), *Cr* I 1.49 20 I
3942.47	2–3	*Fe* I .38 (1), *Fe* I .45 6 IV
3943.58	4	*Fe* I .35 2 IV, *Al* I 4.03 (10)
3945.19	5–6	*Fe* I 4.90 3 IV, *Fe* I 5.12 4 IV
3947.65	1–2	*Fe* I .39 (1), *Fe* I .54 5 IV
3948.79	3	*Fe* I .78 10 IV
3949.95	1–2	*Fe* I .96 10 III
3951.16	2	*Fe* I .17 9 IV
{3952.43, 3953.72}	{v, 4NN, r}	*Fe* I 2.61 8 IV, *Fe* I 2.70 (1), *Fe* I 3.16 4 IV, *Fe* I 3.86 (1)
3955.19	1n	*Fe* I .37 2 IV
3956.57	3	*Fe* I .46 9 IV, *Fe* I .68 12 III
3958.08	2	....
3960.67	2	*Fe* I .29 (1), *Cr* I .77 1 III
3962.15	1	*Fe* I .35 (1)
3963.65	3	*Fe* I .53 (1), *Cr* I .69 30 II
3967.56	3+in $H\epsilon$	*Fe* I .43 8 IV, *Ca* II 8.47 350 II
3970.07	40	$H\epsilon$ .08 (6)
3976.36	7–8	*Fe* I .39 (1), *Fe* I .56 (1), *Fe* I .62 4 IV, *Cr* I .67 25 III
3978.77	1	*Cr* I .69 4 III
3979.50	6	*Fe* I .65 (3) *Cr* I .80 3 III
3981.50	3n?	*Cr* I .24 5 III, *Fe* I .78 7 III
3984.05	4–5	*Cr* I 3.91 20 II, *Fe* I 3.96 10 III, *Cr* I 4.34 10 III
3985.88	3–4	*Fe* I .39 3 IV, *Fe* I 6.18 5 IV
3986.82	4	*Mg* I .79 (4)
3988.91	2	⊙ II 9.00 (3)
3990.55	5–6	*Cr* I 9.99 6 IV, *Fe* I 0.38 2 V
3991.33	3–4	*Cr* I .12 20 II, *Cr* I .68 10 III
3992.62	2–3	*Cr* I .85 15 III
3994.14	4–5	*Cr* I 3.97 4 III, *Fe* I 4.12 2 V
3996.00	1–2N	*Fe* I 5.99 4 IV
3997.26	2	*Fe* I .40 15 III
3998.80	4–5	....

TABLE II—*Continued*

Star	Int.	Identification
3999.76	1	*Cr* I .68 2 V
4000.45	2	*Fe* I .26 (1), *Fe* I .46 2 V
4001.47	2	*Cr* I .45 8 IV, *Fe* I .67 5 III
4002.51	3–4	....
4003.71	3–4	*Fe* I .77 2 V, *Cr* I .92 2 V
4005.03	6	*Fe* I .25 25 II
4006.39	v	
	4NN	*Fe* I 6.31 3 IV, *Fe* I 6.63 2 IV, *Fe* I 6.77 (1), *Fe* I 7.27 6 IV
4007.97	r	
4008.92	1–2	....
4009.60	1–2	*Fe* I .72 10 III
4010.75	2–3	⊙ II .59 (3), *Fe* I .78 (2), *Fe* I .95 (1)
4011.92	2–3	....
4012.46	4	*Ti* II .40 (4), *Cr* I .48 8 IV
4013.78	1–2	*Fe* I .64 (1), *Fe* I .82 2 V
4014.61	3	*Fe* I .54 10 III, *Cr* I .67 3 IV
4015.71	1–2	*Ni* II .50 (1), ⊙ II? .61 (3)
4017.13	3–4	*Fe* I .10 (1), *Fe* I .15 6 III
4017.99	4	*Cr* I 8.22 3 III, *Fe* I 8.28 (2)
4020.19	3n	....
4022.16	4–5	*Fe* I 1.87 12 III, *Cr* I .27 8 IV
4023.54	1	*V* II .38 (50), *Cr* I .74 2 V
4024.72	4	*Fe* I .75 6 V, *Cr* I 5.01 7 III
4025.38	2–3	*Ti* II 5.13 (2)
4026.32	2	*Cr* I .18 10 III
4027.13	1	*Cr* I .11 8 III
4028.40	3	*Ti* II .35 (7)
4030.58	5–6	*Cr* II .37 (pred.), *Fe* I .51 (3) IV, *Mn* I .76 200 I
4032.90	5	*Fe* I 2.64 4 III, *Mn* I 3.07 150 I
4034.26	1	*Mn* I .49 100 I
4035.28	1n	....
4036.21	1	....
4037.20	1–2	*Cr* I .30 3 III
4037.95	2	....
4039.12	3–4	*Cr* I .10 10 III
4040.38	1	*Fe* I .10 (2), *Fe* I .65 4 V
4041.66	1–2n	*Cr* I .81 2 V
4043.92	4–5	*Cr* I .70 3 V, *Fe* I .90 5 IV
4044.65	1	*Fe* I .62 6 IV
4045.86	5	*Fe* I .82 60 II
4047.05	1–2	*Cr* I 6.77 3 IV, *Fe* I 7.32 (1)
4048.11	1	....
4048.99	4–5	*Cr* I .79 10 IV, *Fe* I 9.34 (1)
4049.94	2	*Cr* I .78 2 IV
4052.13	a3–4n	*Fe* I 1.93 (2), *Cr* II .00 (1)
4053.43	1–2	*Cr* II .43 (pred.)
4053.99	3	*Ti* II .84 (3), *Cr* II 4.08 (pred.)
4054.92	2	*Fe* I .83 (1), *Fe* I .88 5n V, *Fe* I 5.05 3 V
4056.15	3	*Cr* I .06 3 V
4057.48	4–5	*Fe* I .36 2 V, *Mg* I .48 (5)
4058.82	2–3	*Fe* I .77 3 IV, *Cr* I .78 10 IV
4059.75	1	*Fe* I .73 3 V
4060.70	2	*Cr* I .67 2 V
4061.82	3	*Fe* I .96 (1)
4063.57	4	*Fe* I .30 (2), *Fe* I .60 45 II, *Cr* II 4.05 (pred.)

TABLE II—*Continued*

Star	Int.	Identification
4065.93.......	1	*Cr* I .72 6 V
4067.08.......	4–5	*Cr* I 6.94 10 III, *Fe* I 6.98 6 III, *Fe* I 7.28 4 III
4068.05.......	2–3	*Fe* I 7.99 8n III
4069.82.......	1–2	....
4070.90.......	3–4	*Fe* I .78 5 III, ?*Cr* II .99 (☉)
4071.74.......	1–2	*Fe* I .75 40 II
4072.67.......	2–3	*Fe* I .51 (1), *Cr* II .63 (pred.)
4073.89.......	1	*Fe* I .76 4n IV
4074.81.......	1–2	*Fe* I .79 5 IV, *Cr* I .86 3 IV
4075.90.......	1–2	*Cr* II .66 (pred.)
4076.87.......	3	*Fe* I .64 8n IV, *Fe* I .81 (1), *Cr* II .88 (pred.), *Cr* I 7.09 5 IV
4077.64.......	4–5	*Cr* II .58 (pred.), *Cr* I .68 4 IV, *Sr* II .71 400 II
4080.16.......	1n	*Fe* I 9.85 4 IV, *Fe* I 0.23 2n IV
4082.25.......	3–4	*Fe* I .12 (1), *Fe* I .44 (☉)
4083.63.......	3	*Fe* I .57 (1), *Fe* I .78 6 IV
4085.25.......	1	*Fe* I .01 4 IV, *Cr* I .02 2 IV, *Fe* I .31 4 IV
4086.06.......	3	*Cr* II .19 (1)
4087.47.......	3	*Fe* II .28 (☉), *Cr* II .61 (pred.)
4088.92.......	2–3	*Fe* I .57 (1), *Cr* II .85 (pred.), *Fe* I 9.22 (1)
4090.23.......	4	*Cr* I .30 3 IV
4092.08.......	1	*Cr* I .18 3 IV
4093.25.......	2	....
4095.04.......	1	....
4096.05.......	1	*Fe* I 5.98 4 IV, *Fe* I 6.12 (1)
4098.09.......	8	*Cr* I $\left\{\begin{matrix}7.65\\7.96\\8.18\end{matrix}\right\}$ 20n III, *Fe* I 8.19 4 IV
4100.30.......	1	....
4101.71.......	30	*Hδ* .74 (7)
4104.20.......	3	*Fe* I .14 3 V
4107.51.......	1	*Fe* I .50 12 III
4109.78.......	1	*Cr* I .58 8 III, *Fe* I .81 9 IV?
4111.15.......	10	*Cr* I $\left\{\begin{matrix}0.87\\1.36\\1.67\end{matrix}\right\}$ 20n III, *Cr* II 1.04 8 III
4112.97.......	8	*Cr* II .57 (pred.), *Fe* I .98 3n V
4114.65.......	1	*Fe* I .45 5 IV
4116.00 }	{ 1–2	....
4116.73 }	{ 1	....
4117.66.......	1	*Fe* I .87 (1)
4118.66.......	2–3	*Fe* I .56 15 IV
4119.54.......	3	....
4121.31.......	2	*Cr* I .27 4 V
4122.63.......	3	*Fe* I .52 4 IV, *Fe* II .67 (*)
4123.55.......	2	*Cr* I .39 10 IV, *Fe* I .76 (1)
4124.64.......	1	....
4125.70 }	{ 1	*Fe* I .63 (1), *Fe* I .89 (1)
4126.20 }	{ 1	*Fe* I .19 3n IV, *Cr* I .52 18 II
4127.18 }	{ 1–2	*Cr* I 6.92 3 III, *Cr* I 7.30 4 IV
4127.84 }	{ 1–2	*Cr* I 7.64 5 III, *Fe* I 7.62 7 IV, *Fe* I .81 3n V
4129.17.......	2–3	*Cr* I .21 20n III
4129.72.......	3	*Eu* II .73 500 III E
4131.09.......	2	*Si* II 0.88 (10), *Cr* I 1.36 10 IV
4132.30.......	7	*Fe* I .06 25 II, *Cr* II .44 (1), *Fe* I .91 8 III

TABLE II—*Continued*

Star	Int.	Identification
4133.92	1	*Fe* I .87 (2)
4134.59	3–4	*Cr* I .39 3 V, *Fe* I .68 12 IV
4135.68	1	....
4137.04	1	*Fe* I .00 7 IV
4138.19	1	....
4139.12	2	....
4140.58	1–2n	....
4142.21	2–3	....
4143.66	6	*Fe* I .42 15 III, *Fe* I .87 30 II
4145.99	6–7	*Fe* I 6.07 (2), *Cr* II 6.50 (pred.)
4147.52	2–3	*Fe* I .68 10 III
4148.51	1	....
4149.36	2	*Fe* I .37 5n IV
4150.74	1	....
4151.84	2	*Fe* I .96 (1), *Fe* I 2.18 4 II A
4152.95	1–2	*Cr* I .78 4 IV, *Cr* I 3.08 4 III
4154.01	3	*Cr* I 3.82 20 III, *Fe* I 3.92 10n IV, *Fe* I 4.11 (1)
4154.68	2	*Fe* I .50 12 III, *Fe* I .82 9 IV
4156.55	4	*Fe* I .81 12 III
4157.73	1	*Fe* I .81 8n IV
4158.87	5	*Fe* I .81 5 V, ⊙ II 9.19 (5)
4161.37	a6	*Cr* I .42 12 IV, *Ti* II .54 (1)
4163.58	4–5	*Cr* I .63 20 III, *Ti* II .65 (40)
4165.51	4	*Fe* I .42 (2), *Cr* I .52 10 IV
4167.28	5	*Mg* I .24 10n III?
4168.74	1	*Fe* I .63(1), *Fe* I .94 (1)
4169.95	3	*Cr* I .84 6 IV, *Cr* I 0.20 4 IV
4170.80	4	*Cr* II .64 (pred.), *Fe* I .91 5 V
4171.92	3	*Ti* II .91 (30), *Fe* I 2.13 5 IV
4172.55	3	*Cr* II .59 (pred.), *Fe* I .75 4 II A, *Cr* II .76 (⊙)
4173.58	2	*Fe* II .48 (5), *Ti* II .55 (1)
4174.88	2	*Cr* I .86 15 III, *Fe* I .92 5 II A, *Cr* I 5.28 3 IV
4175.70	1	*Fe* I .64 10 III
4176.55	1–2	*Fe* I .57 7n IV
4177.81	6	*Fe* I .60 4 II A, *Y* II .61 125 III
4179.20	7	*Fe* II 8.87 (8), *Cr* II .41 (2)
4180.61	1–2	....
4181.77	5	*Fe* I .76 15 III
4184.06	2	⊙ II .00 (4), *Ti* II .33 (0)
4185.16	1–2	*Fe* I 4.89 10 III, *Cr* I 4.90 3 III
4186.36	2	*Cr* I .35 3 IV
4187.75	2	*Fe* I .81 20 III
4188.79	2	⊙ II? .74 (4)
4190.06	2–3	*Cr* I .13 3 IV, *Ti* II .29 (1)
4191.50	6	*Cr* I .27 10 II, *Fe* I .45 15 III, *Fe* I .68 (2)
4192.28	1	*Cr* I .10 5 IV
4193.73	3–4	*Cr* I .66 8 IV
4195.38	5	*Cr* I 4.95 7 III, *Fe* I 5.34 5 IV, *Fe* I 5.62 (2)
4197.21	1	*Cr* I .23 7 IV
4198.30	6–7	*Fe* I .31 20 III, *Cr* I .52 8 IV
4200.60	2N	....
4202.27	3–4	*Fe* I .03 30 I
4204.04	1	*Fe* I 3.95 (1), *Fe* I 3.99 10 III, *Cr* I 4.28 3 III
4205.00	a3–4n	*Y* II 4.69 20 V, *Eu* II 5.05 600 III E

TABLE II—*Continued*

Star	Int.	Identification
4207.18	3	*Cr* I 6.90 4 V, *Fe* I 7.13 4 IV, *Cr* II .34 (pred.)
4208.41	1–2	*Cr* I .35 6 IV, *Fe* I .61 3n V
4209.55	4–5	*Cr* I .36 10 IV, *Cr* I .75 6 III
4211.30	2	*Cr* I .35 6 IV
4212.78	1	*Cr* I .66 4n IV
4213.56	1–2	*Fe* I .65 5 IV
4215.71	10	*Sr* II .52 300 II
4217.58	3–4	*Fe* I .56 7n IV, *Cr* I .63 15 III
4219.44	2–3	*Fe* I .36 12 IV
4220.28	1	*Fe* I .34 4 IV
4222.16	4n	*Cr* I 1.56 8 IV, *Fe* I 2.23 12 III, *Cr* I 2.74 6 III
4224.42	5	*Fe* I .17 6n IV, *Cr* I .51 4 V, *Fe* I .51 3n IV
4227.40	5	*Fe* I 5.46 6n IV, *Fe* I 5.96 3 IV, *Fe* I 6.43 3 IV, *Ca* I 6.73 500 I, *Fe* I 7.45 30 III
4229.84	3–4n	*Fe* I .75 (1) III, *Cr* II .82 (pred.)
4231.60	1	....
4233.21	8–9	*Fe* II .16 (10), *Cr* II .25 (pred.), *Fe* I .61 18 III
4234.58	1	*Cr* I .51 3 III
4236.11	5	*Fe* I 5.95 25 III
4238.74	4	*Fe* I .83 10n IV, *Cr* I .96 8 III
4240.49	2N	*Fe* I .37 (2), *Cr* I .71 10 III
4242.45	7	*Cr* II .39 (5)
4245.24	1	*Fe* I .26 6 III
4246.68	3n	*Fe* I .09 3 V, *Sc* II .83 75 III, *Fe* I 7.44 12 III
4248.49	1	*Fe* I .22 4 IV, *Cr* I .35 2 IV, *Cr* I .72 2 IV
4250.42	5n	*Fe* I .13 25 III, *Fe* I .79 25 II
4252.49	5	*Cr* II .65 (1)
4254.41	6–7	*Cr* I .34 500 II
4256.25	1–2	*Fe* I .21 (2)
4258.19	2N	*Fe* II .16 (*), *Fe* I .39 2 I A
4260.35	6	*Fe* I .14 (2), *Fe* I .49 35 III
4261.93	8	*Cr* II .81 (pred.), *Cr* II .90 (2)
4263.39	1	*Cr* I .14 12 IV
4264.26	2	*Fe* I .21 (2)
4266.40	2n	*Fe* I .97 3 IV
4269.11	6n?	*Cr* II .30 (1)
4271.08	5n	*Fe* I .17 20 III, *Fe* I .76 35 II
4273.37	3–4	*Fe* II .31 (1)
4274.85	2–3	*Cr* I .80 400 II
4275.65	4	*Cr* II .55 (1)
4278.11	a5n	*Fe* II .13 (1), *Fe* I .23 (2)
4280.53	4–5n	*Cr* I .41 12 III
4282.49	3	*Fe* I .41 12 III
4284.39	a4–5	*Cr* II .20 (2)
4285.23	1	*Fe* I .45 3 IV
4288.31	1	*Cr* I? (⊙)
4289.93	6	*Cr* I .73 350 II, *Ti* II 0.22 (50)
4291.89	4–5	*Cr* I .97 6 IV, *Fe* I 2.13 (pred.), *Fe* I 2.29 (1)
4293.95	3	*Ti* II 4.10 (40), *Fe* I 4.13 15 II
4296.71	2–3	*Fe* II .56 (3), *Cr* I 7.06 5 III
4297.94	1–2	*Cr* I .75 12 IV, *Fe* I 8.04 (2) IV
4299.89	7	*Fe* I .25 18 II, *Ti* II 0.05 (60)
4302.09	3	*Ti* II 1.93 (15)
4303.20	3–4	*Fe* II .18 (4)

TABLE II—*Continued*

Star	Int.	Identification
4305.29	3–4n	*Fe* I .46 3 IV, *Cr* I 47 5 III
4306.57	1	....
4307.77	3	*Ti* II .86 40, *Fe* I .91 35 II
4309.31	5	*Fe* I .38 4 IV, *Y* II .61 125 III
4311.23	1	....
4312.78	5	*Ti* II .88 (35)
4314.13	1	*Sc* II .09 100 III
4315.02	5–6	*Ti* II 4.98 (40), *Fe* I 5.09 10 III
4316.86	2	*Ti* II .80 (1)
4318.02	1	*Cr* I? (⊙)
4319.53	4	*Cr* I .65 8 III
4320.98	4N	*Cr* II .60 4 III, *Sc* II .73 75 III, *Ti* II .95 (1), *Cr* I 1.26 3 IV
4323.22	2	*Cr* I .52 5 IV
4325.41	8	*Cr* I .07 15 III, *Fe* I .77 35 II
4328.22	2n?	....
4330.38	3	*Ti* II .26 (0), *Ti* II .71 (0)
4332.74	3	*Cr* I .58 2 IV
4334.50	1	....
4337.75	8	*Fe* I .05 10 II, *Ti* II .32 (1), *Cr* I .57 30 I, *Ti* II .92 (50)
4340.49	25	*H*γ .46 (8)
4344.43	5	*Ti* II .31 (2), *Cr* I .51 40 I
4346.92	1–2	*Cr* I .83 10 III
4348.11	1	*Fe* I 7.85 (1)
4350.03	1	....
4351.80	6–7	*Cr* I .06 20 I, *Fe* I .55 3 IV, *Fe* II .77 (6), *Cr* I .77 60 I, *Mg* I .94 30 IV
4353.95	2–3	*Cr* I .97 2 IV
4357.23	4–5	*Cr* I 6.79 4 III, *Cr* I 7.53 2 III
4359.61	2–3d	*Cr* I .63 20 I
4361.30	1	....
4363.11	4–5	*Cr* I .14 6 III
4366.04	2–3	*Fe* I 5.90 (1)
4367.93	5	*Fe* I .58 5 IV, *Ti* II .66 (15), *Fe* I .91 2 III A
4369.53	2–3	*Fe* II .41 (*), *Fe* I .78 7 III
4371.26	3–4	*Cr* I .28 20 I
4373.43	1	*Cr* I .27 8 I, *Cr* I .65 2 V
4374.57	4N	*Cr* I .16 12 II, *Sc* II .46 60 III, *Ti* II .83 (1), *Cr* I 5.34 8 III
4377.58	1	*Cr* I .55 4 III
4380.87	4	*Cr* I 1.11 6 III
4383.09	2	*Fe* I 2.78 (2), *Fe* I .55 45 II
4384.94	4	*Mg* II .64 (8), *Cr* I .98 20 I, *Fe* II 5.39 (5)
4387.50	3	*Cr* I .38 2 III, *Cr* I .50 5 III
4391.25	4–5n	*Fe* I 0.96 4 IV, *Mg* II 1.58 (10), *Cr* I 1.76 8 I
4395.45	5	*Ti* II .04 (60), *Ti* II .85 (2)
4397.75	2	*Y* II 8.05 100 III
4399.95	2–3	*Ti* II .77 (35), *Cr* I .82 3 III
4401.51	1	*Fe* I .30 (3), *Fe* I .45 (2)
4403.32	4–5	*Cr* I .38 3 III, *Cr* I .50 5 IV
4404.83	2	*Fe* I .75 30 II
4406.74	1	....
4411.76	1	*Ti* II .94 (1)
4413.67 } 4415.22 }	6NN	*Cr* I 3.87 5 III, *Fe* I 5.13 20 II
4416.91	3	*Fe* II .81 (4)

TABLE II—*Continued*

Star	Int.	Identification
4418.25 4419.42	3N	*Ti* II 8.33 (1), *Cr* I 9.11 (☉)
4420.95	1	....
4423.00	10	*Fe* I 2.57 6 III, *Y* II 2.61 80 III, *Cr* I 2.70 2 IV, *Cr* I 3.32 3 III
4424.38	1	*Cr* I .08 2 III, *Cr* I .28 10 III
4427.62	5N	*Fe* I .30 10 I, *Cr* I .72 (☉), *Mg* II .99 (7)
4430.45	7	*Cr* I 9.93 2 IV, *Fe* I .20 (2) IV, *Cr* I 0.48 4 III, *Fe* I .62 6 III
4433.59	3–4N	*Fe* I .22 3n IV, *Mg* II .99 (8)
4435.52 4437.20	1:N	*Fe* I 5.15 (2), *Fe* I 6.93 (2)
4438.71	1	....
4440.88	1	*Fe* I .84 (1), *Fe* I .97 (2)
4443.29	1	*Fe* I .20 7 III
4444.17	5	*Ti* II 3.80 (50), *Ti* II 4.56 (1)
4447.62	3	*Fe* I .73 9 III
4449.45	1	....
4450.50	1	*Cr* I .3 3n IV, *Fe* I .32 (2), *Ti* II .49 (10)
4451.93	1	....
4453.72	1	....
4455.20	1	....
4457.04	2–3	....
4459.02	3	*Cr* I 8.55 12 III, *Ni* I 9.05 20 III, *Fe* I 9.13 10 III, *Cr* I 9.42 4n III
4461.61	5–6	*Fe* I .21 (2), *Fe* I .66 8 I, *Fe* I 2.01 (3) IV
4465.34	a3n	*Cr* I 4.91 4 III, *Cr* I 5.16 2n IV, *Cr* I 5.35 5 III
4466.42	1	*Fe* I .56 12 II
4469.03	2	*Ti* II 8.49 (50), *Ti* II 9.15 (tr), *Fe* I 9.39 5n IV
4472.02	1	....
4474.70 4476.13	3NN	*Cr* I 5.36 8n III, *Fe* I 6.02 10 III
4481.21	10	*Mg* II .13 (100), *Mg* II .33 (100)
4482.76	1	*Cr* I .88 5 III
4484.96	1	....
4488.05	2	*Cr* I .05 5 III
4489.24	2	*Fe* I 8.92 (2) IV, *Fe* II 9.21 (4), *Cr* I 9.47 5 IV, *Fe* I 9.74 3 I A
4491.78	2–3N	*Fe* II .41 (4), *Cr* I .69 3n III, *Cr* I .86 3 III, *Cr* I 2.31 6 III
4495.12	4N	*Fe* I 4.57 12 III, *Cr* I .34 2 IV
4496.94	1	*Cr* I .86 25 I
4499.33		*Cr* I 8.73 6 III
4500.23	4–5N	*Cr* I 0.29 7 III, *Cr* I 1.09 6 III, *Ti* II 1.27 (40)
4501.52		....
4504.24	2	*Cr* II .54 (pred.)
4507.09	3	*Cr* I 6.85 4 IV, *Cr* II 7.23 (pred.)
4508.32	1	*Fe* II .29 (15)
4510.15	1	....
4511.96	3–4	*Cr* I .91 10 III
4514.26	1	*Cr* I .38 (2), *Cr* I .53 8 III
4515.63	5	*Fe* II .34 (15), *Cr* I .44 4 III
4518.13	1	☉ II .34 (1)
4520.24	5	*Fe* II .24 (8)
4522.72	5	*Fe* II .64 (10)

TABLE II—*Continued*

Star	Int.	Identification
4525.01	5	*Cr* I 4.84 2 V, *Fe* I 5.15 5n IV
4526.23	3N	*Cr* I .11 3 IV, *Cr* I .46 15 II
4529.46	1	*Ti* II .49 (1), *Cr* I .69 (3), *Cr* I .76 20 II
4530.89	3–4	*Fe* I 1.16 8 II
4534.23	3n	*Ti* II 3.97 (30), *Fe* II 4.17 (*)
4535.37	3n	*Cr* I .15 6 III, *Cr* I .72 15 II
4538.86	v 5–6	*Cr* I 9.79 5 III, *Cr* I 0.50 12 II, *Cr* I 0.72 10 III, *Cr* I 1.07 5 III
4541.21	r 6NN	
4542.72	1	*Cr* I .52 4 III, *Fe* II .52 (*), *Cr* II .85 (pred.)
4544.58 4546.13	5N	*Cr* I 4.62 12 II, *Cr* II 4.69 (pred.), *Cr* I 5.34 5 III, *Cr* I 5.96 20 I
4549.64	6	*Fe* II .48 (20), *Ti* II .64 (60)
4552.68	2	....
4555.06	5	*Cr* II .09 (10)
4555.77	3	*Fe* II .90 (15), *Fe* I 6.13 4n V
4558.71	8	*Cr* II .66 (20), *Cr* II .78 (pred.)
4561.30	1	....
4563.98	4–5	*Ti* II .76 (30), *Cr* I 4.17 3 V
4565.74	4–5	*Cr* I .51 12 I, *Fe* I .68 (2)
4569.60	2	*Cr* I {.54, .64} 8 III ?
4571.92	4n	*Cr* II .30 (pred.), *Cr* I .68 10 III, *Ti* II .97 (50), *Cr* II 2.87 (pred.)
4573.59	1	....
4576.54	2NN	*Fe* II .31 (10)
4578.01	1:	....
4579.98	3–4	*Cr* I 0.06 20 I
4582.35	1	*Fe* II .84 (*)
4584.02	4N	*Ti* II 3.45 (1), *Fe* II 3.84 (30)
4588.25	7–8	*Cr* II .21 (20), *Cr* II .40 (pred.)
4590.28	2	*Cr* II 9.89 (pred.), *Cr* II 9.96 (pred.), *Ti* II 9.96 (2)
4592.11	4	*Cr* II .06 (4), *Fe* I .66 5 I
4595.80	3–4	*Fe* I .37 (2), *Cr* I .60 6 IV, *Fe* II .70 (*)
4598.31	1–2	*Fe* I .14 (2)
4601.07	2–3N	*Cr* I 0.75 20 I, *Cr* I 1.02 4 III, *Fe* II 1.38 (*)
4602.48	1:	*Fe* I .95 9 I
4604.79	2	*Fe* I .60 (2), *Ni* I .99 12 III
4607.55	1:	*Fe* I .67 3n V
4611.70	1NN	*Fe* I .29 5n III, *Cr* I .97 (2)
4614.42	1	*Cr* I .52 (2)
4616.50	6–7	*Cr* I .14 25 I, *Cr* II .67 (3)
4618.98	7	*Cr* II .82 (10), *Fe* I 9.30 3n IV
4622.12	4–5N	*Cr* I {1.89, 1.96} 10 III, *Cr* I 2.49 5 III
4625.82	5	*Cr* I .93 (3), *Cr* I .19 20 I
4627.52	1:	....
4629.32	2	*Fe* II .33 (20)
4631.72	1	*Cr* I 2.18 2 IV?
4634.35	7N	*Cr* II .09 (10)
4637.90	3	*Fe* I .52 3 IV, *Cr* I .77 4 III, *Fe* I 8.02 3 IV
4639.30 4643.26	2NN	*Cr* I .54 2 IV? *Cr* I .70 (2), *Cr* I 2.01 (2)
4644.23	1	....
4646.69	6–7	*Cr* I .17 40 I, *Cr* I .50 (2), *Cr* I .80 3 IV, *Fe* I 7.44 6 IV

TABLE II—*Continued*

Star	Int.	Identification
4649.03	3N	*Ni* I 8.66 15 III, *Cr* I 8.13 5 III, *Cr* I 8.87 5 IV, *Cr* I 9.46 5 IV
4652.25	2–3	*Cr* I 1.30 20 I, *Cr* I 2.17 30 I
4654.60	3	*Fe* I .50 5 II? *Fe* I .64 5 V, *Cr* I .76 3 IV
4656.86	4	*Cr* I .20 2 IV? *Cr* I .84 (1), *Fe* II .98 (*)
4657.98	2N	....
4661.75	2n	*Fe* I .54 (2), *Fe* I .98 (2)
4663.72	5	*Cr* I .35 7 IV, *Fe* II .71 (*), *Cr* I .85 8 III, *Cr* I 4.81 8 III
4666.74	6	*Cr* I .22 4 III, *Cr* I .52 7 III, *Fe* II .75 (*) *Fe* I 7.46 6 V
4669.81	4–5	*Cr* I .36 6 III
4673.06	5	*Fe* I .17 (3)
4675.03	1:	....
4678.31	2	*Fe* I .86 7 V
4680.69	2	*Cr* I .55 4 III, *Cr* I .87 3 IV
4684.93	4	*Cr* I .61 (1)
4689.11	3N	*Cr* I .40 8 III
4690.35	1:	*Fe* I .15 (2)
4693.68	1	*Cr* I .95 5 III
4695.08	1	*Cr* I .16 3 III
4697.29	2–3	*Cr* I .06 5 III, *Cr* I .40 (1)
4698.89	5–6	*Cr* I $\left\{\begin{matrix}.48\\.62\end{matrix}\right\}$ 20 III, *Cr* I .95 (2), *Cr* I 9.59 (2)
4702.84	2N	*Mg* I .83 (8)
4705.77	1:	*Cr* I 6.10 2 IV
4708.04	5	*Cr* I .06 15 III
4709.97	1	*Fe* I .09 (2), *Fe* I 0.28 5 IV
4714.26	5	*Ni* I .42 25 II
4718.27	4–5	*Cr* I .45 20 III
4720.88	1	*Fe* I 1.00 (1)
4723.26	7	*Cr* I .09 4 III, *Cr* I .41 4 III
4726.96	2:	*Cr* I 7.15 6 III, *Fe* I 7.41 3n IV
4730.94	6	*Cr* I .70 8 III, *Fe* II .49 (1)
4733.90	1	*Fe* I .59 4 IB? *Fe* I 4.10 (1)
4737.21	6	*Fe* I 6.79 12 II? *Cr* I .34 10 III
4740.96	2	*Cr* I 1.09 (1)
4744.80	1	*Cr* I 5.30 2 III
4747.80	4–5	⊙ II 8.14 (4)
4751.68	3N	*Cr* I 2.09 6 IV
4756.89	3N	*Cr* I .13 15 III, *Cr* I 7.35 (1)
4760.51	4n	?*Cr* I 9.92 (1) ?*Cr* I 0.87 (1), *Cr* I 1.26 (1)
4764.89	4:	*Cr* I .31 5 III, *Cr* I .66 1 III, *Fe* I 5.49 (1)
4771.24	3n	*Cr* I 0.69 (1), *Fe* I 1.71 (⊙)
4775.62	4–5	*Cr* I .14 1 (IV)
4779.58	2	*Ti* II .99 (1)
4782.97	4–5	*Cr* I 3.00 (1)
4786.81	4	*Ni* I .54 15 II, *Y* II .57 10 IV, *Fe* I .81 5 IV?
4789.85	3	*Cr* I .35 20 II, *Fe* I .66 7 V, *Cr* I 0.35 2 III A
4792.27	1	*Cr* I .53 15 III
4796.61	2	*Cr* I .17 2 IV
4800.56	1	*Fe* I .65 (2), *Cr* I 1.04 15 III
4805.13	7	*Ti* II .11 (2), *Cr* II .18 (pred.)
4808.70	1	....
4812.38	4	*Cr* II .37 (2)
4816.60	5	....

TABLE II—*Continued*

Star	Int.	Identification
4821.29	2	....
4824.10	6	*Cr* II .13 (10)
4826.90	1	....
4829.44	3	*Cr* I .36 18 II
4833.09	1N	*Fe* I .73 (2)
4836.21	5	*Cr* II .23 (2)
4848.20	6n	*Cr* II .27 (8)
4856.30	4 in $H\beta$	*Cr* II .14 (1)
4861.24	30	$H\beta$ .33 (9)
4871.56	4N	*Cr* I 0.79 20 III, *Fe* I 1.33 25 III, *Fe* I 2.15 20 III
4876.77	5N	*Cr* II .42 (2), *Cr* II .49 (pred.), *Fe* I 8.23 12 III
4881.75	1:	*Fe* I .72 (1), *Fe* I 2.17 (1)
4884.31 } 4887.47 }	6NN	*Y* II 3.70 80 V, *Cr* II 4.61 (1), *Cr* I 4.95 1 III A, *Cr* I 5.77 4 III, *Cr* I 5.95 (2), *Cr* I 7.01 20 II
4890.40	3	*Fe* I .77 25 III, *Fe* I 1.51 50 III
4902.96	5	*Cr* I 3.23 8 III, *Fe* I 3.33 12 III
4920.53	5	*Fe* I 9.01 30 III, *Fe* I 0.52 60 III
4924.11	7	*Fe* II 3.92 (20), *Fe* I 4.78 3 V
4933.97	2:	?*Ba* II 4.10 700 II
4957.68	5	*Fe* I .31 20 III, *Fe* I .61 60 III

NOTES TO TABLE II

The prefix "a" to the intensity denotes that the line is assymmetrical.

4005.03. The wave-length is definitely less than the strong *Fe* I line. There must be an unknown line causing a blend.

4202.27. The wave-length is about a quarter of an angstrom greater than the strong *Fe* I line. Again an unknown line must be disturbing *Fe* I 4202.03.

4224.42–4227.40. The whole interval between these two lines is nebulous.

4861.24. All lines to the red of $H\beta$ are not in good definition and the measures are uncertain.

The Process plate, which is the principal basis for the wave-lengths, was too weak to the red of about λ 4700 to be measurable. The lines of greater wave-length were measured on an Eastman 40 plate.

Al I.—The doublet at 3944 and 3961 is well marked in ϵ Serpentis. The violet component is masked in 73 Draconis and the other member seems to be absent. *Al* I is markedly stronger in ϵ Serpentis.

Si II.—The violet component of the doublet at λ 4128 and λ 4130 is blended in both stars. The red component is unblended and is of intensity 4 in ϵ Serpentis. There is a line of intensity 2 in 73 Draconis at the position of the red component which is a blend of a neutral chromium line with *Si* II. *Si* II is decidedly stronger in ϵ Serpentis.

Ca I.—The ultimate line at λ 4226 contributes about half the intensity to a blend with a strong *Fe* I line in ε Serpentis. On two-prism plates of μ Orionis, an A2 dwarf with a spectrum almost identical with ε Serpentis, the *Ca* I line is resolved from the *Fe* I component, and each line is of intensity 4. In 73 Draconis, *Ca* I 4226, if present at all, contributes to a faint blend. Several other lines of *Ca* I are present in ε Serpentis; no others occur in 73 Draconis. *Ca* I is stronger in ε Serpentis.

Ca II.—The ultimate *Ca* II doublet is very strong in ε Serpentis. The lines are far stronger than any others in the spectrum, with the exception of the Balmer series of hydrogen. In 73 Draconis, K is of intensity 6, fainter than many other lines in the spectrum, and no stronger than several iron arc lines in the neighborhood. There is a greater difference in the intensity of K in the two stars than of any other line. It is weaker in 73 Draconis than in B9 and B8 stars, which contain no *Fe* I lines. As the temperature of 73 Draconis is probably at least as low as that of other A2 stars, there is an indication that the actual abundance of calcium is different.

Sc II.—May be present in both stars but only as components of blended lines.

Ti II.—The lines of *Ti* II at λλ 4501, 4549, and 4571, vary in intensity in 73 Draconis in the period $20^{d}.7$ found for *Eu* II 4205. The amplitude, except in the case of λ 4549, is small. The lines λ 4501 and λ 4571 are blended with chromium, but in each case the principal contributor is *Ti* II. The lines in the neighborhood of λ 4300 were not investigated because a number of the plates were weak in this region and there were no good comparison lines near by. At maximum, *Ti* II is of approximately the same intensity as in ε Serpentis.

V II.—The unblended lines in ε Serpentis at λ 4023 and λ 4035 are of intensity 2. Ionized vanadium is doubtfully present in 73 Draconis. It seems certain that no appreciable part of the variable line at λ 4205 can be due to vanadium.

Cr I.—Only the ultimate lines at λλ 4254, 4275, and 4289 seem to be present in ε Serpentis and the latter two of these are blended. It is possible that one or two of the strongest additional lines may contribute sensibly to the intensities of blends. In 73 Draconis, on

the other hand, all lines in King's list having intensities of 5 or greater are present, as are also a great many lines of lower intensity.

In order that the intensities of the *Cr* I and *Fe* I lines might be compared in 73 Draconis and in the sun, the relation between the Rowland intensity scale and my own was determined by estimating the intensity of a number of unblended lines in a solar spectrum taken with the same instrument and the same kind of plates that were used for the stellar spectra. My estimates for the solar lines were plotted against Rowland's intensities and, as the relation between the two scales was linear, a straight line was fitted to the points. The comparison was made only to intensity 10 on my scale, as the hydrogen lines are the only ones in the case of 73 Draconis

TABLE III

Conversion Table for Intensities of Lines

Int. (Rowland)	Int. (Morgan)	Int. (Rowland)	Int. (Morgan)
2–3	1	6	6
3	2	6–7	7
4	3	7–8	8
4–5	4	8	9
5	5	9	10

whose intensities are greater than 10. The conversion table of my intensity scale to Rowland's is given in Table III.

Except at the lower end, the scales are practically identical. The lines of *Cr* I in 73 Draconis can now be reduced to the Rowland scale and directly compared with the same lines in Rowland's list. Table IV gives the sensibly unblended *Cr* I lines in 73 Draconis and in the sun on the Rowland scale, together with the intensities of the same lines in the sun, the intensities and temperature classes of the lines according to King, and the excitation potentials.

As the Process plate of 73 Draconis deteriorates in quality markedly to the red of λ 4650, the scale of intensities probably also changes, and therefore no lines have been included in Table IV beyond this limit.

There are twelve lines in Table IV for which excitation potentials are available. These lines fall into three groups: (1) the two ultimate lines; (2) five lines with excitation potentials of about 1 volt; and

(3) five other lines with excitation potentials slightly less than 3 volts. If the excitation potentials of these lines are plotted against differences in intensity, 73 Draconis *minus* sun, we obtain Figure 3.

The two ultimate lines are somewhat weakened; those having

TABLE IV

UNBLENDED LINES OF *Cr* I IN 73 DRACONIS AND THE SUN

λ Lab.	Int. 73 Dra. (Row.)	Int. ⊙	Int. Lab.	E.P.
3919.16	4	3	35 II	1.03
3926.65	3-4	0	3 IV	....
3999.68	2-3	−1	2 V	....
4026.18	3	0	10 III	2.70
4027.13	2-3	0	8 III	....
4037.30	3	−1	3 III	2.53
4039.12	4	1	10 III	....
4041.81	3n	−2	2 V	2.53
4049.78	3	(1N d?)	2 IV	....
4056.06	4	0	3 V	....
4060.67	3	(−1)	2 V	....
4065.72	2-3	0	6 V	....
4192.10	2-3	−1	5 IV	....
4193.66	4	0	8 IV	....
4197.23	2-3	0	7 IV	....
4211.35	3	0N	6 IV	....
4254.34	6-7	8	500 II	0.00
4274.80	3-4	7	400 II	0.00
4280.41	4-5n	1	12 III	....
4319.65	4-5	0	8 III	2.88
4332.58	4	0	2 IV	....
4346.83	3	1	10 III	....
4353.97	3-4	0	2 IV	....
4359.63	3-4	3	20 I	0.98
4371.26	4	2	20 I	1.00
4377.55	2-3	0	4 III	....
4381.11	4	0	6 III	2.70
4482.88	2-3	−1	5 III	....
4488.05	3	0	5 III	....
4496.86	2-3	3	25 I	0.94
4511.91	4	1	10 III	....
4580.06	4	3	20 I	0.94
4614.52	2-3	−1	(2)	....

excitation potentials of about 1 volt are very little changed, while the lines of high energy-level are markedly strengthened. When we consider that the temperature of 73 Draconis is around 4000° higher than that of the sun, it is very difficult to account for the presence of the weaker *Cr* I lines. In the case of the normal A2 dwarf ε Serpentis, the ultimate line at λ 4254 has an intensity of about 5 on the Rowland scale, that is, it is of about the same intensity as in 73

Draconis, but the large number of fainter lines which fill the spectrum of 73 Draconis have completely disappeared.

Cr. II—The lines of *Cr* II are at their maximum intensity in 73 Draconis. Even the predicted lines are conspicuous. Ionized chromium is much stronger than in ε Serpentis. As the two stars are of approximately the same temperature, the enhancement of the lines cannot be due to temperature. The pressures in the reversing layers cannot be greatly different, as the wings of the hydrogen lines have about the same appearance. When the abnormal intensity of lines

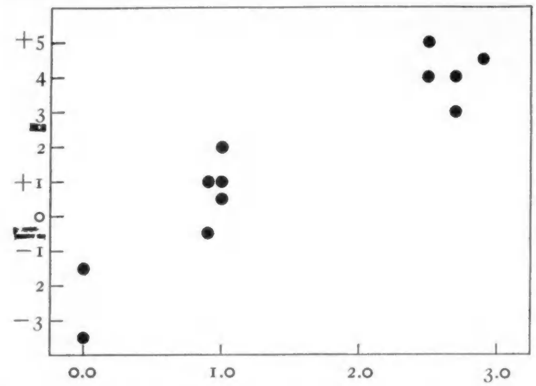

FIG. 3.—Differences in Rowland intensities of *Cr* I lines in 73 Draconis and the sun. Ordinates are differences in intensity in the sense 73 Draconis−sun; abscissae are excitation potentials in volts.

of both *Cr* I and *Cr* II is taken into account, it is difficult to dismiss the possibility of the actual abundance of chromium being different in the two cases.

Mn. I.—The strong ultimate lines at λλ 4030, 4033, and 4034 are present. The first two lines are blended, but the last is apparently free from blends. Neutral manganese is probably slightly stronger in ε Serpentis than in 73 Draconis.

Fe I.—The spectrum of 73 Draconis is dominated by the two elements iron and chromium. Table V gives the sensibly unblended lines of *Fe* I. The columns give: the laboratory wave-length; the intensities in 73 Draconis, ε Serpentis, and the sun, all on the Rowland intensity scale; the laboratory intensity and temperature class according to King; and the excitation potential when known. A separate reduction of the intensities of the lines in ε Serpentis to

TABLE V

UNBLENDED LINES OF *Fe* I IN 73 DRACONIS

λ LAB.	INTENSITY					E P.
	73 Dra.	ε Ser.	Disk	Spot	Lab. T.C.	
3948.78.....	3-4	....	4	3	10 IV	....
3949.96.....	3	....	5	4	10 III	2.17
3951.17.....	3	....	5	4	9 IV	....
3962.35.....	2-3	....	2	1	(1)	....
3995.99.....	3N	....	3	2	4 IV	2.72
3997.40.....	3	Blended	4	(5)	15 III	2.72
4005.25.....	6	11	7	6	25 II	1.55
4009.72.....	3	4n	3	4	10 III	2.21
4044.62.....	2-3	Blended	3	3	6 IV	2.82
4045.82.....	5	12	30	28	60 II	1.48
4059.73.....	2-3	3	2	1	3 V	....
4061.96.....	3-4	Absent	2	1	(1)	....
4063.60.....	4	10	20	15	45 II	1.55
4067.99.....	3-4	4	6	6	8n III	3.20
4071.75.....	3	9	15	15	40 II	1.60
4073.76.....	2-3	3	4	4	4n IV	3.25
4104.14.....	3-4	Absent	5	4	3 V	3.25
4107.50.....	2-3	3	5	5	12 III	2.82
4114.45.....	2-3	3	4	4	5 IV	2.82
4117.87.....	2-3	Absent	2	2	(1)	....
4118.56.....	3-4	Blended	5	5	15 IV	....
4133.87.....	2-3	Absent	3	3	(2)	3.35
4137.00.....	2-3	5	6	5	7 IV	....
4147.68.....	3-4	4	4	6	10 III	1.48
4149.37.....	3	Blended	4	4	5n IV	3.32
4156.81.....	4	Blended	3	3	12 III	2.82
4157.81.....	2-3	3	5	6	8n IV	3.40
4175.64.....	2-3	3	5	5	10 III	2:83
4181.76.....	5	7	5	6	15 III	2.82
4202.03.....	4	8	8	9	30 I	1.48
4219.36.....	3-4	5	4	(7)	12 IV	....
4220.34.....	2-3	3	3	4	4 IV	....
4227.45.....	5	Blended	4	5	30 III	....
4235.95.....	5	8	8	9	25 III	2.42
4245.24.....	2-3	Blended	4	6	6 III	2.85
4256.21.....	3	Absent	1	....	(2)	....
4260.49.....	6	7	10	9	35 III	2.39
4264.21.....	3	Blended	3	3	(2)	3.35
4282.41.....	3-4	6	5	6	12 III	2.17
4285.45.....	2-3	Absent	3	4	3 IV	....
4347.85.....	2-3	Absent	2	3	(1)	3.59
4365.90.....	3-4	Absent	2	2	(1)	2.98
4383.55.....	3	7	15	15	45 II	1.48
4404.75.....	3	7	10	10	30 II	1.55
4443.20.....	2-3	Blended	3	3	7 III	2.85
4447.73.....	3-4	4	6	7	9 III	2.21

NOTE TO TABLE V

Fe I 4005.25 and 4202.03 are shifted about a quarter of an angstrom from their normal positions in 73 Draconis. There is probably an unknown blend causing the shift in wave-length in each case. The lines are not included in the following discussion because the blends seem to be serious.

the Rowland system was made. The published intensities of the lines were corrected by adding two units to bring them to the Rowland system.

In the case of *Cr* I and *Fe* I the material is sufficient to permit a preliminary investigation of the relative number of atoms absorbing lines of various degrees of excitation according to the method developed by Russell, Adams, and Miss Moore.[4] They first calibrated the Rowland solar scale by means of the theoretical intensities of lines in multiplets. As the Rowland intensity scale changes with wave-length, an expression was adopted of the form

TABLE VI

VALUES OF B FOR λλ 3900–4600

λ	B	λ	B
3900	1.16	4300	1.10
4000	1.15	4400	1.08
4100	1.13	4500	1.06
4200	1.11	4600	1.05

$$\log N = B \log A \ ,$$

where N is the number of atoms absorbing a line of a given intensity, B is a function of λ, and A is a function of the Rowland intensity R.

The values of B for λλ 3900–4600 are given in Table VII. Russell and Adams adopted $B = 1.00$ at λ 5000.

In the cases of 73 Draconis and ε Serpentis there will probably be a slight difference in the intensity scale, owing to the change in dispersion along the prismatic spectrum. This has not been allowed for.

As the lines used to transform the arbitrary scales of ε Serpentis and 73 Draconis were chosen in the neighborhood of λ 4200, it was necessary to constuct a table of log A in terms of R for $B = 1.11$ instead of for $B = 1.00$.

The values of log A for $B = 1.11$ are given in Table VII. The values of intensities 2–3 and 3–4 were obtained by linear interpolation.

Values of log N can now be found for the lines of *Cr* I and *Fe* I. For comparison of the relative number of atoms in various states in different stars, the quantity

$$\log \frac{N'}{N} \ ,$$

[4] *Ibid.*, **68**, 271 and 279, 1928.

where N' refers to a star and N to the sun, is computed. For *Fe* I the data permit the sun, 73 Draconis, and ϵ Serpentis to be used. In the sun the values of log A are, of course, the ones given by Russell

TABLE VII

VALUES OF LOG A FOR $B=1.11$

R	log A	R	log A
2–3	1.36	7	3.18
3	1.69	8	3.33
3–4	1.95	9	3.45
4	2.22	10	3.56
5	2.65	11	3.66
6	2.98	12	3.74

and Adams. The twenty-nine sensibly unblended lines in the observed region were used to compute values of log N'/N. The lines in ϵ Serpentis and 73 Draconis were then grouped according to excitation potential and plotted in a manner similar to that used by

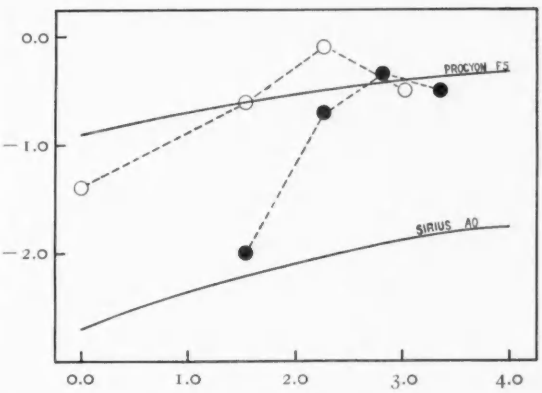

FIG. 4.—Values of log N'/N for *Fe* I for 73 Draconis (closed circles), ϵ Serpentis (open circles), Sirius, and Procyon. The values for Sirius and Procyon are taken from the work of Russell and Adams. Ordinates are expressed in log N'/N; abscissae are excitation potentials in volts.

Russell and Adams. The normal groups are given in Table VIII and the results are shown graphically in Figure 4. A few lines were not observed in ϵ Serpentis which were used in the case of 73 Draconis, and therefore the normal excitation potentials are not the same in the two stars. The curves found from a much more extensive study of Procyon and Sirius by Russell and Adams are also given in Figure 4.

The normal point at excitation potential 0 for ϵ Serpentis has low weight as it depends entirely on one line. The curves in Figure 4 show in another way the remarkable differences in decrement in the intensities of the *Fe* I lines in the two stars having the same spectral type and approximately the same absolute magnitude. Although the

TABLE VIII

NORMAL GROUPS OF LOG N'/N

E.P.	73 Dra.	ϵ Ser.	No. Lines
0.00	....	−1.3	1
1.53	−2.0	0.6	5
2.26	0.7	0.1	6
2.82	0.4	....	10
3.02	....	−0.5	7
3.35	−0.5	....	....

number of atoms in the excited states in the vicinity of 3 volts is about the same, there are twenty-five times as many atoms absorbing the lines of excitation potential 1.5 volts in ϵ Serpentis as in 73 Draconis. An examination of the spectrograms of ϵ Serpentis and 73 Draconis shows that, while the higher subordinate lines are of about the same intensity in the two stars, the low-level lines $\lambda\lambda$ 4045, 4063,

TABLE IX

NORMAL VALUES OF LOG N'/N FOR *Cr* I

E.P.	log N'/N	No. Lines
0.00	−0.73	2
0.98	+0.44	5
2.67	+2.34	5

4071, 4202, 4383, and 4404 are much weaker in 73 Draconis than in ϵ Serpentis. At the present time we have no explanation of this remarkable difference in the spectra of two stars which appear to be physically similar. It is possible that the relative weakness of low-level *Fe* I lines as compared with those of high level is a characteristic of all the peculiar "chromium stars," but further investigation will be necessary before this is established.

From the reduction tables used for iron we can obtain values of log N'/N for *Cr* I. There are twelve lines in Table IV for which

excitation potentials are available. Proceeding in the same way as for *Fe* I, we obtain the normal points shown in Table IX. The columns are the same as for *Fe* I.

These results are shown graphically in Figure 5. For comparison,

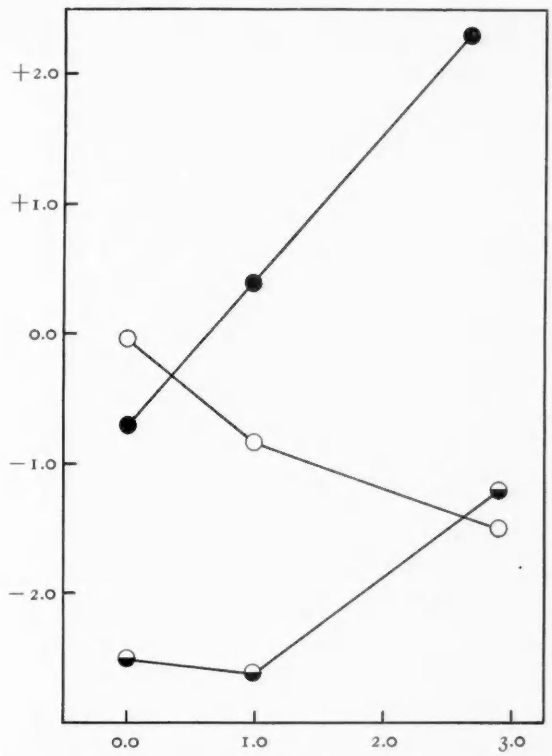

FIG. 5.—Log N'/N for *Cr* I in Sirius (half-closed circles), Procyon (open circles), and 73 Draconis (closed circles). Ordinates are values of log N'/N; abscissae are excitation potentials in volts. The values for Sirius and Procyon are taken from the work of Russell and Adams.

the values found for *Cr* I by Russell and Adams in Sirius and Procyon are also plotted.

Fe II.—The lines of *Fe* II are probably somewhat weaker in 73 Draconis than in ϵ Serpentis. There is not a sufficient range in the excitation potentials of the lines to permit a study similar to that made for *Fe* I.

Ni I.—Neutral nickel seems definitely present in ϵ Serpentis. Its presence is very doubtful in 73 Draconis.

Ni II.—All the classified lines are present in the case of ε Serpentis. The presence of ionized nickel in 73 Draconis is also very doubtful. There can be no doubt that both *Ni* I and *Ni* II are weaker in 73 Draconis than in ε Serpentis.

Sr II.—The ultimate line at λ 4215 is very strong in both stars. It is possible that *Sr* II is stronger in 73 Draconis. The wave-length of this line is shifted slightly toward the violet in the latter star and the line is probably appreciably blended.

Y II.—Ionized yttrium is strong in both stars. The strongest line in the observed spectral range at λ 4177 is of about the same intensity in each spectrum.

Zr II.—All the strongest lines are present in ε Serpentis. The strongest lines are of intensity 5. Ionized zirconium is not present in 73 Draconis.

Ba II.—The ultimate line at λ 4554 is well marked in ε Serpentis. If the line is present at all in 73 Draconis, it is not strong enough to shift appreciably the wave-length of the *Cr* II line which is located 1 A farther to the red. There is, however, a star line near the position of the other strong *Ba* II line at λ 4933 in 73 Draconis.

La II.—Ionized lanthanium seems to be present in ε Serpentis. There are several faint lines which are apparently unblended. There is no evidence for the presence of lanthanum in 73 Draconis.

Eu II.—The two strongest lines at λ 4129 and λ 4205 are present in 73 Draconis. As has been described above, λ 4205 varies in intensity in a period of about twenty days. The line at λ 4129 is too far to the violet to be investigated for variability on the plates available. Ionized europium does not seem to be present in ε Serpentis. None of the other rare earths seems to be present in either star.

The star 73 Draconis is of such exceptional interest that it is being kept on the spectrographic program. It is now possible to obtain spectrograms which extend farther into the violet and much farther toward the red, and I hope to be able to extend the investigation over a wider spectral range than is included here.

Yerkes Observatory
Williams Bay, Wis.
November 8, 1932

VARIATIONS IN STRUCTURE OF THE HYDROGEN LINES IN THE SPECTRUM OF H.D. 31293[1]

By PAUL W. MERRILL and CORA G. BURWELL

ABSTRACT

General description.—The hydrogen lines are very wide and diffuse with intense narrow cores having bright edges on the red side. K is somewhat similar. A few dark lines of *Mg* II and *Fe* II are present.

Measured *displacements* of various lines are given in Tables I and II. Those of the cores of the hydrogen lines vary through a range of 115 km/sec., but the wings remain nearly fixed. Orbital motion does not satisfactorily explain the facts. Atmospheric fluctuations having the same cause as the rapid motions in solar prominences are suggested as a possible alternative.

A bright $H\alpha$ line was detected in the spectrum of this star[2] on an objective-prism photograph taken with the 10-inch telescope on February 18, 1928, and appeared to have approximately the same intensity on a similar plate taken December 23, 1930.[3]

Slit spectrograms taken in our program on bright-line stars showed the hydrogen lines $H\beta$, $H\gamma$, and $H\delta$ to have unusual structures and led to the present brief investigation. The plates listed in Table I were taken with a one-prism spectrograph attached to the 100-inch reflector. All except the first were with the 18-inch camera, giving a dispersion at $H\gamma$ of 38 A per millimeter.

A strong absorption core with sharp edges dominates $H\beta$, $H\gamma$, and $H\delta$ (see Pl. III). A bright fringe toward the red is conspicuous at $H\beta$ on most of the plates, but is always weak at $H\gamma$ and $H\delta$. It varies in intensity. Wide wings of low intensity complete the structure. The dark K line is strong, with a well-defined minimum; the structure probably resembles that of $H\delta$, although the wings are less intense, and emission fringes are not seen. The dark magnesium line λ 4481 is narrow and measurable with fair accuracy. Dark lines of ionized iron are very weak and ill-defined. A grating spectrogram of the visual region, taken on September 19, 1932, shows $H\alpha$

[1] *Contributions from the Mount Wilson Observatory, Carnegie Institution of Washington,* No. 462.

[2] H.D. 31293, B.D.+30°741; 1900 R.A. $4^h49^m.4$, Dec.+30°24′; mag. 7.5; spectrum Harvard Ao, Mt. Wilson Aoep.

[3] *Mt. Wilson Contr.,* No. 456; *Astrophysical Journal,* **76,** 156, 1932.

to be a strong bright line, somewhat displaced toward longer wavelengths, with a wide relatively weak absorption line on the violet side. D1,2 of sodium and D3 of helium are weak or absent.

The measured displacements of the lines are in Table I. The cores of $H\gamma$ and $H\delta$ apparently give the same values within errors of measurement; hence their mean value, μ, alone, is tabulated. The mean displacement ranges from -11 to -126 km/sec. and, as the

TABLE I

DISPLACEMENTS IN KM/SEC.

Plate	Date	J.D. 2420000 +	$\frac{H\gamma+H\delta}{2}=\mu$	$H\beta$ Abs.	$H\beta$ Em.	λ 4481	$\frac{H+K}{2}$
C 5020*.......	1928 Oct. 3	5523	− 46	− 71	+138	....	(−41)
5024........	Oct. 4	5524	60	79	96	− 8	(−46)
5057........	Oct. 31	5551	92	114	85	+37	....
5101........	Dec. 21	5602	82	107	108	+13	(−38)
5144........	1929 Mar. 1	5672	53	93	95	+27	−27
5309........	Sept. 13	5868	11	67	147	+29	−20
5332........	Oct. 9	5894	85	84	79	+ 9	(−47)
5352........	Nov. 20	5936	48	53	109	+21	−35
5370........	Dec. 13	5959	50	48	110	−26	−29
5401........	1930 Feb. 12	6020	79	93	104	−14	−46
5548........	Sept. 10	6230	126	125	91	+ 2	....
5613........	Nov. 12	6293	61	64	82	+16	(−24)
5638........	Dec. 3	6314	60	49	111	−12	(− 7)
5643........	Dec. 4	6315	− 14	− 26	+145	+10	(+ 7)

* Ten-inch camera. All other plates with 18-inch camera.

last two plates show, is subject to quick changes. The varying displacements may or may not be caused by orbital motion, but we should consider it expedient to list this object as a spectroscopic binary.

The displacement of the dark core of $H\beta$ shows a curious relationship to μ. The plates may be divided, without changing their chronological sequence, into three fairly homogeneous groups as tabulated:

Plates	$H\beta-\mu$
Nos. 5020–5101............	−22 km/sec.
5144–5309............	−48
5332–5643............	− 2

The displacements of $H\beta$ (and to a less degree the values of $H\beta-\mu$) show a loose correlation with the intensities of the emission

PLATE III

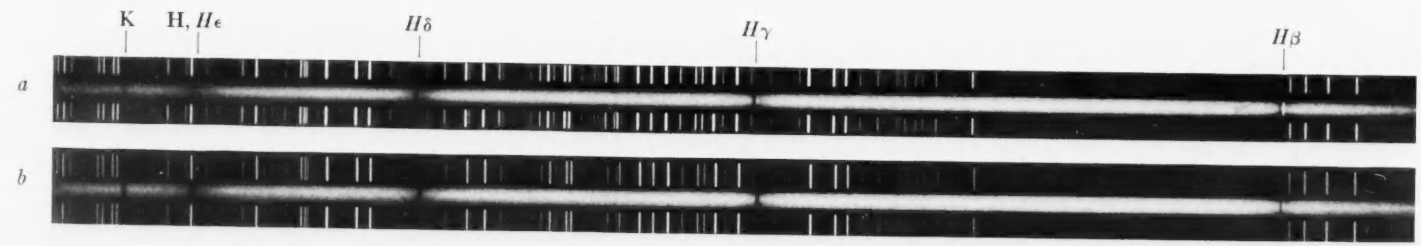

SPECTROGRAMS OF H.D. 31293

a) C 5101, 1928 December 21
b) C 5643, 1930 December 4

component $H\beta$ Er in which increased emission accompanies algebraically small displacements.

The iron lines and magnesium λ 4481 yield displacements algebraically larger than μ by 70 km/sec., while H and K give intermediate values. Mean displacements of various lines are in Table II.

The displacements of H and K show a correlation with μ, although their range is less and their mean value higher. The cause of the peculiar behavior of the hydrogen lines thus seems to affect H and K in a similar but less pronounced fashion. This fact is difficult to explain on the hypothesis of orbital motion. The displacements of λ 4481 appear not to depend on μ, nor do they show a correlation

TABLE II

MEAN DISPLACEMENTS OF VARIOUS LINES

μ	− 62 km/sec.
$H\beta$a	− 77
H, K	− 29
λ 4481	+ 8
Fe II	+ 7
$H\alpha$ Er	(+ 64)
$H\beta$ Er	+107
$H\gamma$ Er	+ 91
$H\delta$ Er	(+ 81)

with those of *Fe* II lines. The behavior of λ 4481 is clearly different from that of the cores of the hydrogen lines, but the apparent scatter with *Fe* II lines might be caused by errors of observation.

Figure 1, in which the displacements of various lines are plotted against the time, exhibits graphically several facts already noted. The intervals separating the plates are apparently too great to bring out satisfactorily the true nature of the displacement-curves. Observations every night would be desirable for this purpose.

Inspection of the negatives revealed changes in the structure of the hydrogen lines and suggested that the wings are more nearly stationary than the cores, which, as the measures show, are subject to widely different displacements (see Table I). This interesting phenomenon has been confirmed by a brief study with the microphotometer of plates C 5057, C 5309, and C 5548 (see Fig. 2). Tracings of $H\gamma$ and $H\delta$ on each plate were superposed in turn on the

corresponding curves of each of the other plates, the wings being placed as nearly in coincidence as possible; the distance between the cores was then measured. This gave two values of the relative displacement of core and wing for a line on each pair of plates. The measurements were then repeated, the rectified curves, i.e., those

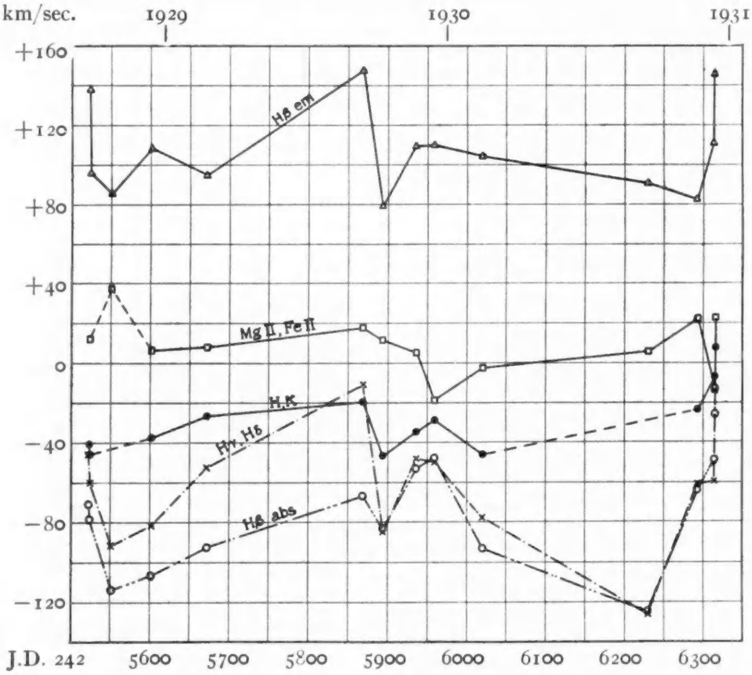

FIG. 1.—Displacements of spectral lines plotted against time

in which the continuous spectrum on each side of the line is brought to the same density, being used. The four values so found are in Table III.

The measured displacement of the cores was smaller on C 5309 than on the other two plates, and the lines appeared more nearly symmetrical. For purposes of comparison we assume, therefore, that on this plate the wings have the same displacements as the core.[4] Table IV gives the results of applying to the measured displacements

[4] The slight error which this assumption may involve will not vitiate the results because we are finding merely the *changes* in the position of the wings which accompany the measured changes in the position of the core.

of the cores the differential displacements of the wings from Table III. The displacements of the core are the μ values from Table I converted into angstrom units. The approximate constancy of the first group of values in the last two columns compared with the

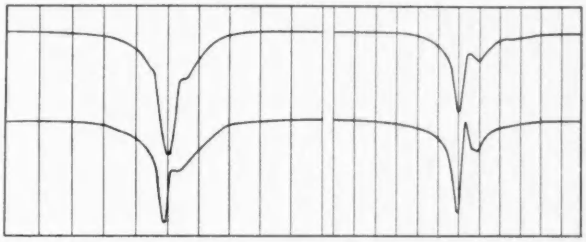

FIG. 2.—Intensity-curves sketched from microphotometer tracings. Upper, C 5309, 1929 September 13; lower, C 5548, 1930 September 10; left, $H\gamma$; right, $H\beta$.

range in the preceding columns shows that *the wings do not move with the core,* but remain nearly fixed in position. In view of the agreement of the values for $H\delta$,[5] the indication that the wings of $H\gamma$ move by small amounts oppositely to the core cannot be relied

TABLE III

RELATIVE DISPLACEMENTS OF WING AND CORE
(Angstrom units)

	C 5057–C 5309		C 5548–C 5309		C 5548–C 5057	
	$H\gamma$	$H\delta$	$H\gamma$	$H\delta$	$H\gamma$	$H\delta$
	−1.4	−1.0	−2.4	−2.5	−1.0	−0.8
	1.4	1.2	2.2	1.0	0.4	0.4
	1.7	1.3	2.2	1.3	0.3	0.0
	−1.5	−0.9	−2.0	−1.5	−0.1	−1.0
Means..	−1.50	−1.10	−2.20	−1.58	−0.45	−0.55

upon. The last two lines of Table IV, based on a similar direct comparison of plates C 5057 and C 5548, show the wings to have remained fixed within errors of observation while, in this instance, the cores moved about 0.5 A.

The residual intensities (percentages) in the cores of the hydrogen lines on the last two plates were found to be as tabulated. The re-

[5] Their exact agreement to 0.01 A is a coincidence.

sults for $H\delta$ are uncertain; the true values may be less than those given.

	$H\beta$	$H\gamma$	$H\delta$
C 5638	24	13	(15)
C 5643	22	8	(8)

The extreme widths of the lines cannot be stated with accuracy because it is impossible to determine exactly the point at which the photometric curve begins to fall below the level of the continuous spectrum. For $H\gamma$ and $H\delta$, however, the widths are of the order of 65 A.

TABLE IV

DISPLACEMENTS OF CORE AND WINGS

(Angstrom units)

PLATE	CORE		WING	
	$H\gamma$	$H\delta$	$H\gamma$	$H\delta$
C 5309	−0.16	−0.15	(−0.16)	(−0.15)
C 5057	1.33	1.25	+0.17	0.15
C 5548	1.83	1.73	+0.37	0.15
C 5057	1.33	1.25	(−1.33)	(1.25)
C 5548	−1.83	−1.73	−1.38	−1.18

The low residual intensities at the minima of the hydrogen lines make improbable the assumption that the cores are produced by one star while the wings and certain other lines come from a companion body. The large range in the displacements of the core combined with the nearly fixed positions of other lines is also unfavorable to this assumption. Another strong argument against it is the fact that the range in the velocities from H and K is less than that from the hydrogen cores, while the mean velocity is intermediate between that from the cores and from other lines (see Fig. 1).

Rejection of the binary hypothesis, however, leaves us in a predicament, for we must then imagine the atoms producing the core to have high and rapidly changing velocities with respect to the lower and nearly stationary layers responsible for the wings and the lines of other elements. Such motions must not be considered totally impossible, however, for they are of frequent occurrence in

solar prominences. Indeed, a curious parallelism between typical features of Be spectra and certain phenomena of the solar chromosphere indicates a degree of similarity between the physical conditions in atmospheres of Be stars and those in the chromosphere and prominences and suggests, by way of speculation, that the (unknown) cause of rapid motion in prominences may perhaps, in stars hotter than the sun, be sufficiently powerful and well organized to produce observable effects in the spectrum of the integrated light.

The spectrum of H.D. 31293 is one of a number of early-type spectra with emission lines in which changes in the complex structure of the hydrogen lines accompany displacements of the core.[6] This behavior is important in the general problem of bright lines in stellar spectra, and related phenomena may, in some stars, be involved in the structure and displacements of lines without recognized emission.

NOTE ADDED TO PROOF

We have just noticed that H.D. 31293 is identical with AB Aurigae, a variable of the R Coronae type.[7] The recent light-curve is not at hand, but it seems probable that our spectrograms were taken at or near the constant maximum brightness.

Carnegie Institution of Washington
Mount Wilson Observatory
October 1932

[6] The spectrum of H.D. 163296 is remarkably similar in appearance and behavior to that of H.D. 31293 (*Mt. Wilson Contr.*, No. 409; *Astrophysical Journal*, **72**, 98, 1930).

[7] *Harvard Bulletin*, No. 798, 1924.

THE VARIATION IN THE RADIAL VELOCITY OF α ORIONIS FROM 1923 TO 1931[1]

By ROSCOE F. SANFORD

ABSTRACT

Mean radial-velocity variation.—The radial velocities of α Orionis obtained at Mount Wilson between 1923 and 1931 show a mean long-period variation whose times of maximum and minimum are represented by Jones's elements, but whose amplitude exceeds his by 50 per cent. Variations within shorter intervals do not appear to be periodic.

Relation between mean light and mean velocity variation.—The mean curves are so related in phase that the pulsation theory would require that maximum light coincide with minimum radius and minimum light with maximum radius. The change in radius would be of the order of 114.5×10^6 km, or about 30 per cent on either side of the most probable median radius. Measures of the diameter with the stellar interferometer have extreme values which are in harmony with this result, but are too few to establish with certainty a periodicity in the change.

When individual observations are considered, changes in radial velocity are not consistently related to changes in light except in the case of the most pronounced of the secondary fluctuations, when the velocity decreases as the light increases and vice versa.

Temperature and spectral class.—The surface temperatures computed from the apparent visual magnitudes and the radii at maximum and minimum of light are reasonably close to those associated with the first few subdivisions of spectral class M. The spectrum appears always to contain the bands of titanium oxide and to undergo little if any change. The indicated change in radius and magnitude requires a surface brightness at maximum which is about five times that at minimum.

J. Stebbins[2] has recently published a series of observations of the brightness of α Orionis extending from 1908 to 1931, made with selenium and photoelectric cell photometers at the Universities of Illinois and Wisconsin. He finds measurable changes in brightness, not infrequently rapid enough to be associated with a period of less than a year, although no single period seems to represent them, and he is inclined to regard these variations as irregular. The reality of a longer period may be fairly well established, however, by grouping each season's observations into a normal place and assembling the normals in a single cycle. A least-squares solution gave 5.4 years for the period. H. S. Jones[3] had found 5.781 years to be best suited to the radial velocities available to him. Stebbins considers this

[1] *Contributions from the Mount Wilson Observatory, Carnegie Institution of Washington,* No. 464.

[2] *Publications of the Washburn Observatory of the University of Wisconsin,* **15,** 177–191, 1931.

[3] *Monthly Notices of the Royal Astronomical Society,* **88,** 660, 1928.

period and concludes that it does nearly as well for his own observations, that it represents the Cape and Lick Observatory radial velocities used by Jones, and, finally, that it is required by practically all the important long series of visual estimates of the light. Jones's period is therefore assumed to be correct. Stebbins' data furnish a good mean light-curve and also a fairly detailed continuous record covering the twenty-three-year interval, both of which are of particular interest in what follows.

Spectrograms of α Orionis with high dispersion have been obtained at Mount Wilson since 1923, partly because of the interest attaching to its curious variations of radial velocity and partly to have a record of their values concurrent with measures of angular diameter with the stellar interferometer. The resulting radial velocities may now be considered in connection with Stebbins' observations and mean light-curve and Pease's measures of the diameter with the interferometer. The forty-four spectrograms (Table I) suitable for the determination of radial velocity were obtained partly with a three-prism spectrograph attached to the 60-inch (dispersion, 5.1 A per millimeter at $H\gamma$)[4] and partly with various auto-collimating spectrographs used with the 100-inch reflector in coudé form (2.9–5.0 A per millimeter).

The measured radial velocities depend on a group of about sixty lines selected to minimize the effect of blends as much as possible. Since these effects cannot be avoided entirely, corrections were necessary, especially for those spectrograms on which it was not possible to measure all the lines of the group. The mean velocity for a spectrogram reduced with the *Revised Rowland* wave-lengths for all the lines is probably substantially correct, since the effect of blends on different lines of this group is accidental. Average systematic deviations from the mean velocity formed for the individual lines from a number of plates afforded a basis for the necessary corrections. A comparison of the corrected wave-lengths with those taken from the *Revised Rowland* shows a mean difference of less than 0.01 A. Furthermore, the agreement of the velocities derived from individual lines on a single plate is as good as can be expected with the dispersion used.

[4] *Mt. Wilson Contr.*, No. 59; *Astrophysical Journal*, **35**, 163, 1912.

The individual velocities of Table I are plotted in Figure 1*a* as ordinates against the Julian dates of observation. Three-prism plates are represented by crosses; coudé plates by encircled crosses. In addition, Lick Observatory[5] velocities obtained since 1920 are indicated by dots and open circles, the latter representing results with low dispersion. Lick Observatory spectrograms taken since

TABLE I

MOUNT WILSON RADIAL VELOCITIES OF α ORIONIS

Plate No.	J.D.	Vel.	Plate No.	J.D.	Vel.
		km/sec.			km/sec.
γ 11437*.....	2423365.968	+21.3	Coudé 5...	2424597.701	+18.9
11495......	3422.721	23.9	46...	4807.000	15.4
11496......	3422.766	23.3	47...	4835.920	16.1
12169......	3696.009	22.9	59...	4879.833	16.1
12170......	3696.035	23.9	62...	4903.696	18.1
12194......	3713.940	23.2	66...	4914.690	16.4
12294......	3747.849	20.9	γ 15377...	5189.950	19.4
12324......	3769.803	23.6	15465...	5248.756	21.8
12325......	3769.828	22.6	15466...	5248.806	22.4
12401......	3802.661	21.9	15616...	5314.627	22.8
12402......	3802.687	21.9	15667...	5343.622	23.0
12497......	3834.620	21.7	Coudé 123...	5592.883	27.0
13092......	4100.810	20.2	127...	5609.876	22.8
13129......	4131.802	18.3	138...	5613.816	20.5
13184......	4159.658	18.6	162...	5696.712	23.7
13254......	4191.679	15.7	211...	5906.966	23.7
13255......	4191.710	16.8	219...	5929.848	21.0
13717......	4403.014	19.6	231...	5932.863	23.7
13893......	4480.936	19.2	243...	5966.906	21.8
13897......	4482.961	19.1	350...	6252.963	18.0
13929......	4508.888	21.1	365...	6290.930	19.3
13991......	4537.790	+22.7	419...	6603.992	+18.6

* Plates of the γ series are with the three-prism spectrograph and 60-inch reflector.

1926 have been kindly lent to me by Dr. Moore. The velocities (the third column of Table II) are from my own measures reduced with the system of wave-lengths used for the Mount Wilson spectrograms and corrected for flexure. There is no evidence of any appreciable systematic difference between these results and those obtained from the earlier spectrograms which were reduced at the Lick Observatory. Both the Lick and the Mount Wilson measures show that variations of considerable range may take place in a single season. This has been the usual result whenever the star has been

[5] *Publications of the Lick Observatory*, **16**, 81, 1928.

observed with adequate dispersion. No simple period appears to represent these changes, which sometimes occupy an interval as short as two hundred days and sometimes as much as five hundred

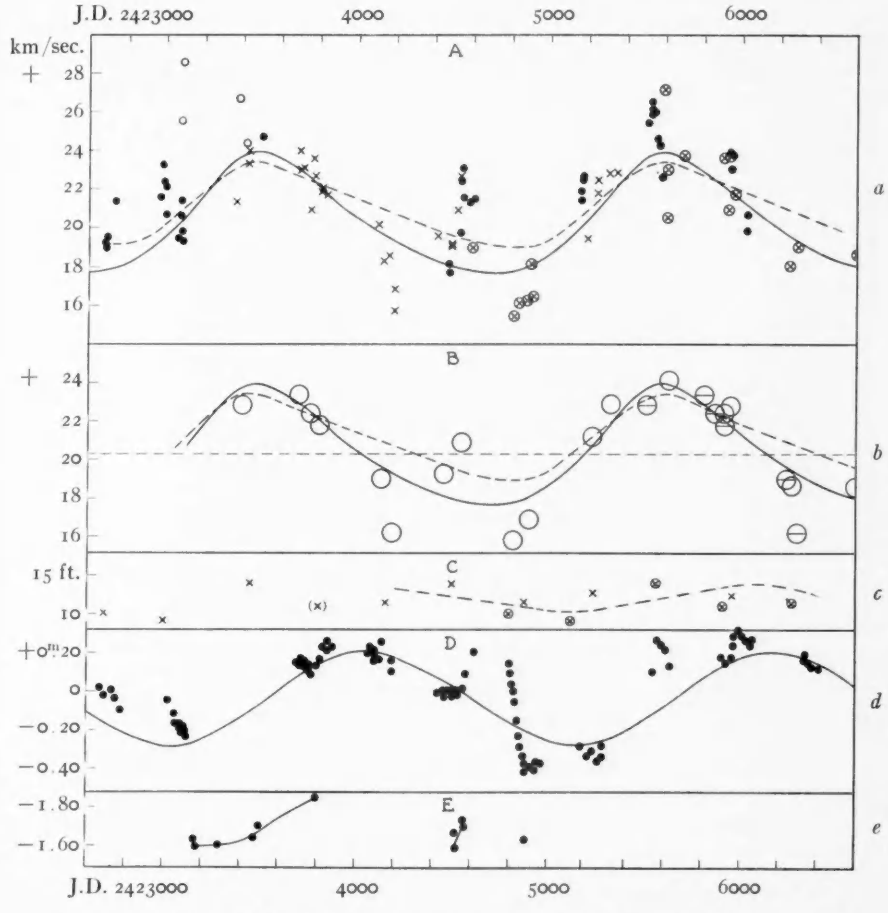

FIG. 1.—(*a*) individual radial velocities of α Orionis as abscissae against Julian dates as ordinates. Dots and circles, Lick Observatory observations, 1920–1931. Crosses (three-prism spectrograms) and encircled crosses (coudé spectrograms), Mount Wilson observations, 1923–1931. (*b*) Mount Wilson normal places. In both (*a*) and (*b*) the broken-line curve is from Jones's elements, the other from the Mount Wilson elements which define the γ velocity represented by the broken horizontal line in (*b*). (*c*) Pease's observations with interferometer for determination of star's diameter. (*d*) Stebbins' individual determinations of magnitude and his mean light-curve. (*e*) Nicholson and Pettit's radiometric magnitudes for α Orionis.

days. The outstanding high values from Lick Observatory represented by circles might be attributed to the low dispersion used; but coudé plate 123, which is of excellent quality, gives an almost equally high value.

It is also evident from Figure 1*a* that the velocities follow a variation covering several years which is marked by fairly definite maxima and minima. The broken curve in Figure 1*a* based on Jones's elements (Table IV) shows general agreement in the observed and predicted maxima and minima and is further justification for adopting a period of 5.781 years.

TABLE II

LICK OBSERVATORY OBSERVATIONS AFTER 1926

No.	Julian Day	Vel.	No.	Julian Day	Vel.
		km/sec.			km/sec.
15735	2425164	+21.4	16242	2425561	+24.6
15736	5164	21.9	16257	5571	24.3
15764	5176	22.5	16299	5587	22.6
15768	5177	22.6	17032	5945	23.8
16138	5513	25.5	17033	5945	23.8
16157	5528	26.6	17045	5948	23.1
16175	5536	25.9	17141	6025	19.8
16185	5537	26.1	17142	6025	+20.7
16197	5539	+26.0			

In order to show more clearly the long-period variation in the Mount Wilson radial velocities, normal places have been formed by combining not more than four consecutive values, which in no case cover an interval much exceeding one hundred days. The mean values are given in Table III and plotted as circles in Figure 1*b*. The barred circles are a repetition of normal places preceding J.D. 2424200, brought forward one period. For convenience, the normal places have been represented by the orbital motion of a spectroscopic binary, although it is not suggested that such is the real explanation. The elements, which, exclusive of the period, were once corrected by least squares, are given in Table IV.

The continuous curve in Figure 1*b* is defined by the Mount Wilson elements, the broken-line curve by Jones's elements, as also in Figure 1*a*. The maxima and minima of the two radial-velocity

curves agree closely. The amplitudes, however, are 6.16 km/sec. for Mount Wilson and 4.12 km/sec. for Jones, and a glance at Figure 1*b* shows that the larger amplitude is necessary for the representation of the normal places. A possible explanation is a variation in the amplitude, the mean for the several cycles used by Jones being less than that for the 1923–1931 observations. The residuals for the normal places are, however, larger than those to be expected from individual observations if only a smooth variation is involved. Presumably, therefore, the effect of the shorter fluctuations has not been smoothed out completely by forming normal places.

TABLE III

NORMAL PLACES FOR α ORIONIS

No.	Julian Day	Vel.	Plates Involved
		km/sec.	
1	2423404	+22.8	γ 11437, 11495, 11496
2	3702	23.4	γ 12169, 12170, 12194
3	3762	22.4	γ 12294, 12324, 12325
4	3813	21.8	γ 12401, 12402, 12497
5	4131	19.0	γ 13092, 13129, 13184
6	4192	16.2	γ 13254, 13255
7	4456	19.3	γ 13717, 13893, 13897
8	4548	20.9	γ 13929, 13991, C 5
9	4821	15.8	C 46, 47
10	4899	16.9	C 59, 62, 66
11	5228	21.2	γ 15377, 15465, 15466
12	5328	22.9	γ 15616, 15667
13	5627	24.1	C 123, 127, 138, 162
14	5918	22.4	C 211, 219
15	5950	22.8	C 231, 243
16	6271	18.7	C 350, 365
17	6603	+18.6	C 419

TABLE IV

ORBITAL ELEMENTS OF α ORIONIS

	Jones	Mount Wilson
Period	5.781 yrs.	5.781 years (assumed)
K	2.06 $\pm$0.09	3.08 $\pm$0.42 km/sec.
e	0.208$\pm$0.039	0.200$\pm$0°069
ω	285°8 $\pm$11°1	322°7 $\pm$24°4
T	1904.97 $\pm$.18 yrs. =	J.D.2425444.7$\pm$77ᵈ9 =
	1928.09$\pm$18 yrs.	1928.545$\pm$0.21
γ	+21.05 km/sec.	+20.33 km/sec.
$a \sin i$	58,500,000 km	81,773,000 km

Stebbins' observations of α Orionis during 1920–1931 inclusive are shown in Figure 1*d*, together with his mean light-curve. The ordinates (magnitude differences) are positive when α Orionis is brighter than the mean of the comparison stars.

Although individual measures do not consistently follow the curve, their departures are no more pronounced than those of individual radial velocities from the mean velocity-curve. Nicholson and Pettit have kindly placed at my disposal some radiometric measures of α Orionis made with the thermocouple. Although not numerous, they are of interest in confirming some of Stebbins' results (Fig. 1*e*). From J.D. 2423200 to 2423800 they show the steady increase observed by Stebbins, and the few between J.D. 2424500 and 2424900 are consistent with the irregularity in Stebbins' measures marked by the rise from a quiescent stage to a secondary maximum at about J.D. 2424700 and followed by a decline to a minimum at J.D. 2424900. During this interval the radial velocities ranged from a secondary maximum to a secondary minimum, perhaps somewhat before J.D. 2424800, after which they increased rapidly at the time when the light was rapidly waning to the secondary minimum at J.D. 2424900. There is, however, no general correlation between light and velocity of the kind suggested by these individual observations. For example, the rapid change in radial velocity in the interval J.D. 2424100–2424200 occurred at a time when the brightness was remarkably constant. The radial velocities and the photometric measures all show deviations from the mean curves which can scarcely be ascribed to errors of observation. Their interrelation apparently can be unraveled, if at all, only by a large number of observations of all kinds extending over several years.

Stebbins concluded that velocity minimum for the period of 5.781 years follows light maximum by 1.5 years. Comparison with the Mount Wilson mean velocity-curve shows an even larger interval. In fact, maximum light occurs very nearly at the time when the diminishing radial velocity becomes equal to the velocity of the system. Further, minimum of light is just as closely related to the instant when the increasing velocity equals the velocity of the system. The relation between the mean light- and velocity-curves is

therefore neither that of an eclipsing binary nor that of an ordinary Cepheid variable.

Much has been made in recent years of the theory of pulsating stars, especially in explaining the light variations of Cepheids. It is interesting to note how the light and velocity variations of α Orionis fit into such a theory. If its observed variation in radial velocity results from pulsation, the maximum and minimum diameters should be reached as the radial velocity referred to the center of the star changes sign. These changes occurred near J.D. 2425190 (maximum diameter) and J.D. 2426140 (minimum diameter). These dates are close to the times of light minimum and maximum, respectively. In other words, the assumption of pulsation leads to the conclusion that the star has its least diameter at maximum light, and vice versa. Moreover, the value of $a \sin i$ (from the elements), increased by about 40 per cent to allow for oblique rays from the star's limb, is roughly a measure of the change in radius undergone by a pulsating star.[6] For α Orionis this quantity amounts to 114.5×10^6 km.

TABLE V

Year	Separation of Mirrors	Angular Diameter	Reference
1920.9	10 ft.	0".047	*A.S.P. Pubs.*, **34**, 346, 1922
1921.9	8.5	.054	*Ibid.*
1922.9	14	.034	*Ibid.*
1924	(11.5)*	....	*Annual Report Mt. Wilson Observatory*, 1924
1925	....	.044	*Ibid.*, 1925
1926	14	....	*Ibid.*, 1925–1926
1927	11.5	....	*Ibid.*, 1926–1927
1928	12.7	....	*Ibid.*, 1927–1928
1930	....	0.040	*Ibid.*, 1930–1931

* Pease gives low weight to this measure.

These results raise a question as to the evidence furnished by direct measures of the angular diameter of the star. Pease's published measures with the stellar interferometer are in Table V. The extreme values are 0".034 and 0".054. With a parallax of 0".017 ± 0".004 the mean (0".044) corresponds to a linear radius 279 times that of the sun, or 196×10^6 km.

[6] *Proceedings of the National Academy of Sciences*, **5**, 422, 1919; Russell, Dugan, and Stewart, *Astronomy*, **2**, 767, 1927.

The extreme values measured give, similarly, 246×10^6 and 146×10^6 km for the maximum and minimum radii, respectively, or a difference of 100×10^6 km, which is to be compared to 114.5×10^6 km given by the radial velocities. The two values, representing a fluctuation of about 30 per cent on either side of the mean radius, agree surprisingly well when all the uncertainties upon which they rest are considered.

The interferometer measures given in Table V have been plotted in Figure 1*c* as mirror separations against Julian dates of observation. All values previous to J.D. 2424200 have been carried forward one period (5.781 years) and entered as encircled crosses. The result is not very definite, but the minimum mirror separation (maximum diameter) seems to be not far from minimum light. It is difficult to infer the course of the curve for mirror separation through the remaining observations, but they are as well represented by a maximum near light maximum as by any other arrangement involving a simple curve with a period of 5.781 years. Curve 1*c* agrees with the radial-velocity curve in making the maximum radius correspond with light minimum and the minimum radius with light maximum. The curve is, however, so uncertain that its evidence is far from satisfactory.

If maximum light really corresponds to minimum radius, and vice versa, the surface brightness at maximum light must be nearly five times that at minimum light in order that an area 0.3 that at minimum shall have a magnitude that is 0.4 brighter.

The superficial absolute temperature of a star is given by[7]

$$T=\frac{5900^\circ}{3.05+0.20m+\log d}\ ,$$

where m is the visual apparent magnitude and d the angular diameter in seconds of arc. For

$$m=0.7\ ,\qquad d=0\overset{''}{.}034\ \text{(maximum light)}\ ,$$

$$m=1.1\ ,\qquad d=0.054\ \text{(minimum light)}\ ,$$

[7] Russell, Dugan, and Stewart, *op. cit.*, 2, 749, 1927.

we find $T = 3430°$ and $2950°$ for maximum and minimum, respectively, and $3190°$ for the median temperature. Normally, the maximum and minimum values would correspond[8] approximately to spectral types gK5 and gM3. For such a difference in spectrum there would probably be detectable differences in both the lines and the bands. Since the lines do not seem to change and the bands of titanium oxide are always present, the spectrum is at all times apparently of class M. Small changes in the intensity of the bands corresponding to a few tenths in spectral class are not, however, excluded. Further, the spectrograms give no trustworthy evidence as to changes in the effective wave-length which might be expected to accompany so large a variation in surface brightness. Although the computed temperature change would in the mean indicate a spectral variation of the amount given, it is not greater than the dispersion in temperature among individual early class-M stars, and the spectrograms do not exclude the small spectral changes which might account for such a temperature range.

Carnegie Institution of Washington
Mount Wilson Observatory
September 1932

[8] *Ibid.*, p. 753.

ON THE SPECTRUM AND RADIAL VELOCITY OF U MONOCEROTIS[1]

By ROSCOE F. SANFORD

ABSTRACT

Radial velocities.—Spectrograms of U Monocerotis over the interval 1922–1932 show a variation of 40 km/sec. in the center of mass velocity in a period of about 2300 days. The change from lowest to highest velocity occupies two-thirds of this period.

When the observed radial velocities are corrected for the foregoing long-period variation and then plotted with the best period available from photometric data, a velocity variation with a total amplitude of 23 km/sec. is obtained. This variation has double maxima and minima and a period of 92.26 days. The velocity of the system is +34.6 km/sec.

The enhanced lines are displaced to the red of the arc lines by an amount equivalent to a velocity of 5 km/sec. Blends no doubt affect this result. The emission lines of hydrogen, when present, give a displacement of 39 km/sec. to the violet.

Relation of changes of light, velocity, and spectral class.—The phases for the latest spectral class and other associated features are followed in a very few days by the phases of light minima, which in turn slightly precede the velocity maxima. A similar order exists for the epochs of earliest spectral class, light maxima, and velocity maxima. Coincidence of light maxima and velocity minima, and vice versa, is, however, possible because of some uncertainty as to the exact phases of the extremes of velocity. The latest spectral class appears to occur when the radial velocities are on the increase, whereas the earliest spectral class goes with a decrease; but there is no definite relation to the termination of velocities of approach or of recession.

Gould describes the discovery and early observations of U Monocerotis[2] in the following words:

> The magnitude of this star, which I have designated as U Monocerotis, was noted by Lalande as 8, and by Bessel as 6; but the limits of its fluctuation appear to be approximately 6.0 and 7.2. A continuous series of estimates was made by Mr. Thome in 1873 from April 21 to June 14; showing maxima about April 20 and June 5, and a minimum on May 14. Another maximum must have occurred not far from 1874 Jan. 18, on which date the magnitude was estimated as 6.0.
>
> The period is about 46 days and minimum somewhat nearer to the preceding than to the following maximum.[3]

The numerous photometric observations throughout the remainder of the nineteenth century[4] include the work of such experienced observers as Espin, Sawyer, Pickering, Yendell, Markwick,

[1] *Contributions from the Mount Wilson Observatory, Carnegie Institution of Washington*, No. 465.

[2] B.D. $-9^\circ 2085$; A. G. Wien-Ott 2696; Boss 1970; H.D. 59693; (1900) $\alpha = 7^h 26^m\!.0$, $\delta = -9^\circ 34'$.

[3] *Resultados del Observatorio Nacional Argentino*, **1**, 333, 1875.

[4] Müller and Hartwig, *Geschichte und Literatur des Lichtwechsels*, **1**, 228, 1918.

Dawson, Pereira, Hartwig, Hisgen, and Luizet. Observations of comparatively recent date have been made by E. Loreta[5] and F. Lause.[6]

Much of this work reveals a variation of light intimately related to the 46-day period first found by Thome. But as time went on and series of observations covering longer intervals accumulated, it became evident that the variation did not strictly follow this period and was best interpreted as that of the RV Tauri type. This conclusion required that Thome's period be doubled. There are, therefore, within this longer interval two maxima and two minima. Further, U Monocerotis, like other variables of this class, undergoes changes involving the depths of the minima and the heights of the maxima. At times the minima may be nearly equal, or either one may be the fainter. It is not known whether these changes are recurrent in some long period or whether they follow no fixed law. D. B. McLaughlin,[7] who has studied the light variations of the RV Tauri variable R Scuti, concludes that "the irregularities of R Scuti are themselves related in a regular manner." Since this star, which has hitherto been considered about the most irregular member of its class, seems after all to conform to law, other RV Tauri stars may, on intensive study, also prove regular. Meanwhile the period best suited to the existing data on U Monocerotis appears to be 92.26 days.

Radial velocities.—U Monocerotis is one of the brightest of the RV Tauri variables and hence as favorable as any for spectroscopic study. Table I lists 51 one-prism spectrograms, with a dispersion of about 37 A per millimeter at $H\gamma$, obtained at Mount Wilson with the 60-inch (γ series) and 100-inch (C series) reflectors. Seven of these were obtained between 1922 and 1927, after which the seasons are successively represented by observations as follows:

	Spectrograms
1927–1928	4
1928–1929	5
1929–1930	8
1930–1931	14
1931–1932	13

[5] *Bulletin de l'Observatoire de Lyon,* **11,** 46A, 1929.

[6] *Astronomische Nachrichten,* **239,** 59, 1930; **244,** 79, 1931.

[7] *Publications of the Observatory of the University of Michigan,* **4,** 135, 1932.

TABLE I

RADIAL VELOCITIES OF U MONOCEROTIS

Plate No.	J.D. 2420000+	Phase	Vel.	Corr.	Corr. Vel.
			km/sec.	km/sec.	km/sec.
γ 10725......	3060.893	−68[d]	+33.8	− 4	+30
10902......	3126.726	− 2	27.3	+ 6	33
11485......	3419.956	+14	26.6	+18	45
12344......	3773.978	− 8	29.1	+15	44
12444......	3810.785	+36	18.2	+14	32
14133......	4604.697	0	39.6	−11	29
14865......	4957.753	−16	56.4	−22	34
C 4573......	5222.933	−28	49.3	+ 3	36
γ 15592......	5285.803	−57	48.2	−10	38
15604......	5306.722	−36	43.9	− 7	37
15606......	5310.675	−33	37.1	− 7	30
16365......	5609.867	−10	29.5	+15	45
16375......	5611.803	− 8	25.1	+15	40
16389......	5613.851	− 6	21.9	+15	37
C 5154......	5700.672	−11	21.3	+18	39
γ 16505......	5703.635	− 9	19.9	+18	38
17029......	5907.035	+10	14.1	+17	31
17098......	5936.015	−53	33.5	+17	51
17141......	5961.992	−27	20.0	+16	36
17169......	5969.868	−19	28.2	+16	44
17174......	5981.829	− 7	28.8	+16	45
17263......	6023.701	−57	22.6	+14	37
17342......	6054.648	−26	24.9	+13	38
C 5437......	6082.659	+ 1	15.5	+13	28
γ 17809......	6262.987	− 3	26.6	+ 7	34
C 5581......	6266.027	0	26.5	+ 7	34
γ 17840......	6282.975	−75	32.7	+ 7	40
γ 17871......	6288.036	−71	34.4	+ 7	41
17896......	6293.989	−65	33.2	+ 7	40
17906......	6310.999	−48	9.9	+ 6	16
17948......	6316.963	−42	17.1	+ 6	23
17966......	6320.926	−38	9.9	+ 6	26
17977......	6322.931	−36	25.5	+ 6	31
17987......	6335.914	−23	38.1	+ 6	44
C 5675......	6342.901	−16	33.4	+ 6	39
γ 18032......	6345.885	−13	33.7	+ 6	40
18053......	6374.749	+17	34.3	+ 6	40
18075......	6402.645	−48	20.9	+ 5	26
V 65*.....	6640.021	+ 5	18.0	− 1	17
γ 18554......	6663.935	−64	38.6	− 1	38
18559......	6664.930	−63	41.8	− 1	41
18594......	6676.997	−51	35.2	− 1	34
18603......	6693.893	−34	28.2	− 2	26
18628......	6706.828	−20	43.7	− 2	42
18638......	6723.883	− 4	33.4	− 3	30
18669......	6731.751	+ 5	39.0	− 3	36
18684......	6736.780	+10	35.0	− 3	32
18697......	6758.674	−61	36.2	− 4	32
C 5968......	6762.789	−57	40.8	− 4	37
γ 18776......	6793.653	−26	37.7	− 4	34
C 5985......	6796.687	−23	+31.3	− 4	+27

* Obtained with three-prism ultra-violet spectrograph and 10-inch camera; dispersion 23 A per millimeter at H and K.

The radial velocities in the fourth column of Table I were obtained by reducing the measures with the Mount Wilson tables for arc lines applicable to spectral class G. The observations are not numerous enough for a dependable study of differences in the behavior of the radial velocities during successive or closely adjacent cycles, but considerable information of interest comes out of the mean results. The following discussion compares the light-curve, the velocity-curve, and the curves showing various spectral changes.

The period of 92.26 days obtained from the photometric data represents the radial velocities as well or better than any other and

TABLE II

Approximate J.D.	Systematic Deviation
2423100	(+ 4) km/sec.
3420	(+ 9)
3780	(+15)
4610	(−10)
4960	(−24)
5260	−10
5670	+17
6000	+15
6380	+ 5
6700	0

was therefore adopted. The phases for the spectrograms were reckoned arbitrarily from J.D. 2426727 G.M.T. The plotted observations of 1931–1932 define a curve complete enough to serve as a normal with which the run of the observations for the other seasons may be compared. Such a comparison leaves little doubt that the velocity of the system changes from season to season. From 1922 to 1927 the data are meager, but for the remaining seasons the evidence is in each instance based upon several spectrograms and merits considerable confidence. The estimated systematic deviation of each season's observations from the adopted normal of 1931–1932 (normal—seasonal) is shown in Table II, values of low weight being inclosed in parentheses.

An attempt to represent these deviations by a smooth curve is given in Figure 1. The more uncertain portion depending upon the first five values in Table II is indicated by a broken line which near

the crest has purposely been made to conform more or less to the shape of the next crest, which appears to be well defined. A period of about 2300 days is thus revealed, during which the center-of-mass velocity as seasonally determined varies through 40 km/sec., the change from lowest to highest values lasting about two-thirds of the period. Quite by accident the zero velocity corresponds closely to the axis which divides the curve into two equal areas. It follows, therefore, that the velocity of the center of mass may be found from the 1931–1932 observations alone, or from all the observations when they have been corrected for the variation displayed in Figure 1.

The measured velocities in the fourth column of Table I have

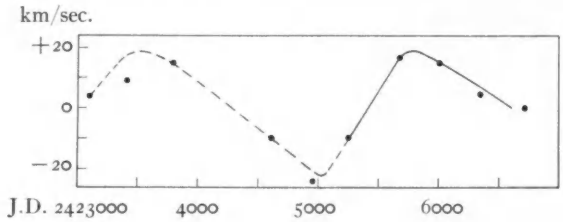

FIG. 1.—Variation in center-of-mass velocity (normal, 1931–1932—seasonal). Abscissae and ordinates from first and second columns, respectively, of Table II.

been corrected by the quantities in the fifth column scaled from Figure 1. The corrected values in the last column are shown graphically in Figure 2*a*, where the abscissae are the phases from the third column of Table I. Although the scatter is still somewhat greater than would be expected from the errors of observation and measurement, two maxima and two minima of slightly different value are evident. The free-hand curve taken to represent the general course of the velocity variation has an extreme range of only about 23 km/sec. The difference in the maxima is perhaps open to doubt, but that in the minima seems certain, the minimum at phase 44 days being definitely the deeper.

Since the velocities in Table I are numerous, small in range, and rather even in distribution, the velocity of the center of mass of U Monocerotis may be obtained by taking the straight mean of all the quantities in the last column of the table. The result is +34.6 km/sec., and is represented by the broken horizontal line in Figure

2*a*, which fulfils the condition that the areas under the velocity-curve above and below this line are approximately equal.

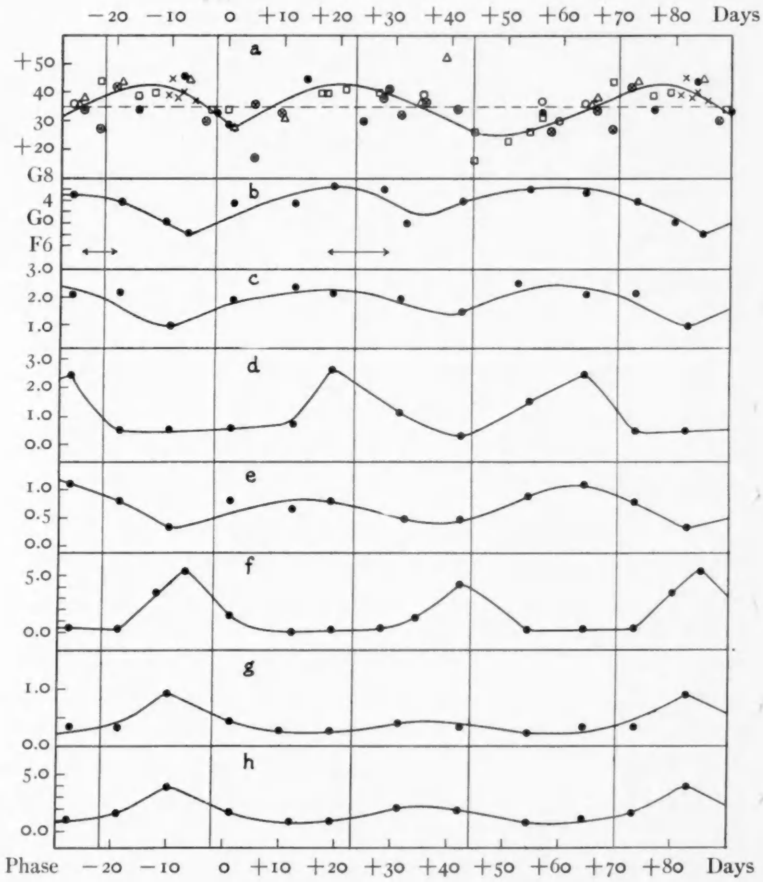

FIG. 2.—(*a*) Corrected velocities (abscissae) from sixth column and phases (ordinates) from third column of Table I. Dots, the seven observations of 1922–1927. The other seasons are successively represented by circles, crosses, triangles, squares, and encircled crosses. The broken horizontal line shows the velocity of the system.

The remaining curves indicate the changes in (*b*) type, (*c*) the G band, (*d*) $H\gamma$ in absorption, (*e*) λ 4408, (*f*) $H\gamma$ in emission, (*g*) λ 4321, and (*h*) λ 4344. The phase intervals for bands of titanium oxide are shown by short horizontal lines below (*b*). The vertical lines show the mean phases for maxima and minima of light.

In addition to the arc lines, some enhanced lines have been measured upon a large percentage of the spectrograms. The lines

are relatively few, however, and the blends so serious that in many cases velocities for individual plates computed from enhanced lines alone would be rather uncertain. It seemed better, therefore, to collect all the residuals for the enhanced lines relative to the mean arc-line velocity appropriate to each plate and then form the mean for the entire series. This procedure utilized all the available data, gave no undue weight to a velocity difference from a spectrogram on which few enhanced lines had been measured, and, furthermore, in effect weighted each line in accordance with the number of times it was measured. This mean difference is equivalent to a Doppler shift of $+5$ km/sec. relative to the velocities from the arc lines. The writer's estimate for the similar difference in the case of AC Herculis,[8] another RV Tauri variable, is $+6.9$ km/sec. The effect which blends may have in producing such a difference is, however, recognized and attention called to it.

At certain phases (to be discussed later), $H\delta$, $H\gamma$, and $H\beta$ of hydrogen appear as emission lines. Ten values of the radial velocity from these lines, depending for the most part upon $H\gamma$, are available and show without exception a velocity of approach (if interpreted as a Doppler shift) relative to that found from the arc lines. The mean of the ten differences (emission − arc) lines is -39 km/sec. It is probable that a very faint emission component having a positive displacement relative to the arc lines is sometimes present, but this was not sufficiently certain to warrant measurement. AC Herculis[9] showed both emission components during a short interval, but the violet member was usually the stronger, persisted much longer, and gave a mean displacement of about -65 km/sec.

Comparison of light and velocity changes.—The data for the light variation of U Monocerotis are so heterogeneous that the task of bringing them all to a common system appeared unjustified. The recent observations of Loreta and Lause, already referred to, fall within the interval covered by the radial velocities and might therefore be preferred as a source from which to get the phases of maximum and minimum light. The mean values thus found (reckoned as for the radial velocities) appear in the second column of Table

[8] *Mt. Wilson Contr.*, No. 424; *Astrophysical Journal*, **73**, 364, 1931.

[9] *Ibid.*

III. Mean values have likewise been computed from all the available photometric data, beginning with the first observations by Thome (Table III, col. 3). Although there is a considerable spread in the individual determinations, it is not enough to confuse the two maxima or the two minima. The agreement between the two series is surprisingly good, and the values based upon the complete data have therefore been adopted. The designations are those of Lause, but it should be remarked that the primary minimum in his first series became the secondary minimum in his second, an example of the RV Tauri type of light variation that this star undergoes.

The vertical lines in Figure 2 represent the four adopted phases. There is a rough though none too certain correspondence between

TABLE III

PHASES OF MAXIMA AND MINIMA

Designation	Phase (Loreta and Lause)	Phase (All)
Maximum 2	0^d (92^d)	90^d
Minimum (principal)	23	23
Maximum 1	46	44
Minimum (secondary)	70	70

the light minima and velocity maxima, and the light maxima and velocity minima. The correspondence for the principal minimum and maximum 1 is good, but for the other two cases the radial velocities appear to lag. On account of the uncertainty involved, it is perhaps justifiable to accept the correspondence tentatively. The low velocity minimum at phase 44 days rests almost wholly upon the radial velocities obtained in 1930–1931. The most outstanding single observation is γ 17098 of the preceding season. It may be significant that Lause's light observations show the secondary minimum for this latter season to be the brighter, whereas in 1930–1931 it was the fainter of the two minima.

Spectral class.—The spectrograms were compared on the Hartmann spectrocomparator with a series of Cepheid variables which had been previously classified. The intensities of a number of enhanced lines were also compared with neighboring lines which vary little with type or in the opposite way to the enhanced lines. The

intensity of the G band, which varies to a noticeable degree, was estimated on an arbitrary scale for each spectrogram. The presence of bands of titanium oxide was noted in a few cases. The hydrogen lines change from strong absorption lines, through a stage in which the lines are practically obliterated, to fairly strong emission. A measure of this change was obtained by estimating the strength of the emission and by comparing the intensity of the hydrogen line in absorption with a neighboring absorption line. The individual values so obtained during the various spectral changes are subject to considerable range; smoothed results have therefore been obtained by taking the means within phase intervals of ten days.

The succession of curves below the velocity-curve in Figure 2 are defined by these means for the changes observed in (*b*) spectral class; (*c*) the G band; (*d*) $H\gamma$ in absorption; (*e*) the intensity of λ 4408 (strong in class-M stars) as compared with the neutral iron line λ 4404; (*f*) $H\gamma$ in emission; (*g*) the intensity of λ 4321 Ti^+, Sc^+; and (*h*) the intensity of λ 4344 Ti^+. The comparison line for λ 4321 was λ 4318 *Ca*, *Ti*, and for λ 4344 the line λ 4347 *Fe*. Both these comparison lines are themselves subject to change, but in a direction opposite to that of the enhanced lines. Curves (*g*) and (*h*) are therefore only differential and probably more pronounced than if the comparison could have been made with lines that varied little in a cycle. Casual inspection of the spectrograms shows, however, that at least a part of the change indicated by the curves is inherent in the enhanced lines. Two horizontal lines below the curve for spectral class indicate the phase intervals within which titanium oxide bands were observed.

These curves agree in giving approximately the same values for the two phases which correspond to the latest spectral class, the strongest G band, the strongest hydrogen lines in absorption, the weakest enhanced lines, and the strongest λ 4408. Likewise two phases are consistently indicated for the earliest type, the weakest G band, the strongest emission lines of hydrogen, the strongest enhanced lines, and the weakest λ 4408. The mean values for the latest spectral class and other associated features are phases -29^d and $+19^d$, and for the other two, pertaining to early type, phases -7^d and $+36^d$. The phases in Table III which correspond most

closely are -22^d and $+23$ for the first pair and -2^d and $+44^d$ for the other pair. It follows that the latest spectral class and its related characteristics precede the light minimum, while the earliest type precedes light maximum by a mean interval of approximately six days. The curves seem to agree in showing a lag in the light-curve relative to the curves of spectral type. The titanium oxide bands (horizontal lines beneath Fig. 2*b*) appear, however, in both cases somewhat after the time of latest spectral class, and the intervals of their duration are symmetrical with respect to the phases of the two minima. A. H. Joy[10] has noted that these bands occasionally appear at certain phases in the spectra of some of the variable stars of intermediate periods, although the general line spectrum is not so late as that usually associated with stars of class M. P. W. Merrill[11] has also found that the bands appear at times in certain stars of spectral class S. There is therefore evidence that these bands are not uniquely associated with a specific absorption-line spectrum. Hence, the appearance of titanium oxide bands after the latest type is attained is not necessarily an indication that the spectral classification here given is uncertain by an amount that would correspond to the lag in phase.

When the radial-velocity curve is considered, it may be stated that the latest spectral class occurs on the rising branches and the earliest on the falling branches, but with no very close relationship to the intersection of the γ-axis with the curve of Figure 2*a*.

CARNEGIE INSTITUTION OF WASHINGTON
MOUNT WILSON OBSERVATORY
October 1932

[10] *Mt. Wilson Contr.*, No. 443; *Astrophysical Journal*, **75**, 127, 1932.

[11] *Mt. Wilson Contr.*, No. 252; *Astrophysical Journal*, **56**, 457, 1922; *Mt. Wilson Contr.*, No. 325; *Astrophysical Journal*, **65**, 23, 1927.

ON THE MODIFICATION OF THE INTENSITY DISTRIBUTION IN THE BAND SPECTRUM OF NITROGEN

By J. OKUBO and H. HAMADA

ABSTRACT

The modification of the intensity distribution of the nitrogen band spectrum by changes of temperature, pressure, exciting voltage, and current, and the shape of the discharge tube, was observed. From the results obtained in this experiment, it is found that the better defined and sharper the selective enhancements of the bands with the vibrational quantum numbers $v' = \sim 6$ and $v' = \sim 11$ in the first positive bands, and with $v' = \sim 0, 1$ in the second positive as well as in the negative bands, are observed, the lower the temperature of the gas, and the smaller the density of the exciting current. It is also found that this effect is observable conspicuously in the first and the second positive bands, and weakly in the negative bands. It has been confirmed that the selective enhancements of the bands above described are always observable, independently of the exciting conditions, so long as the exciting current density is small and the temperature of the gas is low. In the case of a very low pressure, i.e., when the velocities of the impacting electrons are relatively high, the bands from the initial levels with the higher vibrational quantum numbers are relatively enhanced in the three band systems here investigated, as G. Herzberg has already confirmed, and the maximum in the band group tends to be displaced toward the band with greater v'. In conclusion, some considerations regarding the results obtained and some references to the band spectrum of nitrogen in the auroral spectrum have been added.

INTRODUCTION

It is generally accepted that, of the α bands of active nitrogen, those emitted by the transitions from the initial levels with the vibrational quantum numbers $v' = \sim 6$ and ~ 11 in the upper $B^3\Pi$ state of nitrogen molecules are especially enhanced.[1] However, it has also been found that the enhancement of these bands is observed not only in the case of active nitrogen but also in other cases of the excitation of nitrogen molecules.

G. Herzberg[2] has already investigated the intensity distribution of the first and the second positive as well as the negative bands of nitrogen, and has satisfactorily interpreted the results on the Franck-Condon principle. In the following pages the results of observations of the modifications of this intensity distribution of the nitrogen band spectrum by the changes of temperature, pressure, exciting voltage and current, and the shape of the discharge tube

[1] G. Cario and J. Kaplan, *Zeitschrift für Physik*, **58**, 769, 1929.

[2] *Zeitschrift für Physik*, **49**, 761, 1928.

will be described; some considerations regarding the results obtained and some reference to the band spectrum of nitrogen in the auroral spectrum will also be added.

EXPERIMENTAL RESULTS

The excitation of nitrogen molecules was carried out on one occasion in a glass bulb 25 cm in diameter, and on another in a tube about 1 cm in diameter, and tubes of other dimensions have also been used. The gas was excited by a current from a high-tension direct-current dynamo, or by a condensed, as well as an uncondensed, discharge from an induction coil, and, in the case of the direct current, the current density was varied in the range between 20 milliamp/cm^2 and less than 0.1 milliamp/cm^2. The pressure of the gas was also varied from a few mm to one-hundredth of a mm, and the spectrum was observed at three different temperatures, namely, at room temperature, at 650° C, and at the temperature of liquid air. The spectrograph used was made by the Franz-Schmidt and Haensch Company, the photographic plate was an Agfa Panchromatic, and, in photographing the spectrum in the infra-red region, it was sensitized with "Illuminol U II" made by the Institute of Physical and Chemical Research in Tokyo. For the sake of comparison, the spectra emitted, under various conditions of excitation, were photographed side by side on the same plate, and the variation of the relative intensities of the bands due to the changes of excitation conditions were studied.

In the first place, the effect of the temperature variation of the gas will be described. At the temperature of liquid air, in the first positive bands, selective enhancements with the vibrational quantum numbers[3] $v'=\sim 6$ and $v'=\sim 11$ in the upper $B^3\Pi$ state were observed relative to the other bands of the same group, that is, the bands at 5593 (6,1), 6070 (6,2), 6624 (6,3), 7273 (6,4), 8047 (6,5), 5407 (11,6), and 5804 (11,7) appear sharply enhanced, and it is also known that the more intense the enhancements of the bands observable, the nearer are the vibrational quantum numbers in the initial levels to $v'=6$ and $v'=11$ (Pl. IV*a*). In this case, the bands with $v'=\sim 6$ are always more enhanced than those with $v'=\sim 11$, which

[3] E. Angerer, *Annalen der Physik*, **32**, 549, 1910.

is quite contrary to the intensity distribution in the α bands of active nitrogen. It is also observable that the bands at 7753 and 8722, which are emitted by the transitions from the vibrational level $v' = 2$ in the upper $B^3\Pi$ state, are slightly enhanced at liquid air temperature relatively to the other neighboring bands. Similar modifications of intensities of the bands are observable in the second positive, as well as in the negative, bands, and in these band systems it was found that those emitted by the transitions from the initial levels corresponding to the lower vibrational quantum numbers ($v' = 0,1$) are relatively enhanced.

In the case of the high temperature of 650° C, the selective enhancements of the intensities of the bands become very small, and all the bands tend to be emitted with nearly the same intensity. Of the first positive bands, those with the initial vibrational quantum numbers greater as well as less than $v' = 6$ and $v' = 11$ are both enhanced (Pl. IV*b*), while of the second positive and the negative bands those with the initial vibrational quantum numbers v' greater than 0 or 1 are relatively enhanced. It should also be noted here that the modification of the intensity distribution in the band system accompanying the variation of temperature is most considerable in the first and the second positive bands, while it is weakest in the negative bands.

In the second place, the modifications of the intensity distribution of the band system due to the variation of the exciting current density were observed. In the first positive bands, the more sharply enhanced the observed appearance of the bands with $v' = \sim 6$ and $v' = \sim 11$, the smaller the current density. These selections are markedly sharp in the case of a current density less than 0.1 milliamp/cm², but in the case of such a feeble current it is impossible to measure exactly the current density, as the discharge does not take place uniformly over the whole section of the tube. By increasing the current density, the sharpness or distinctness of such selections is lost and all the bands tend to appear with nearly equal intensity. The bands with $v' = \sim 2$ are also somewhat enhanced relatively in the case of the lower current density.

Similar modifications of intensities were also observed in the second positive as well as in the negative bands. In the former band

PLATE IV

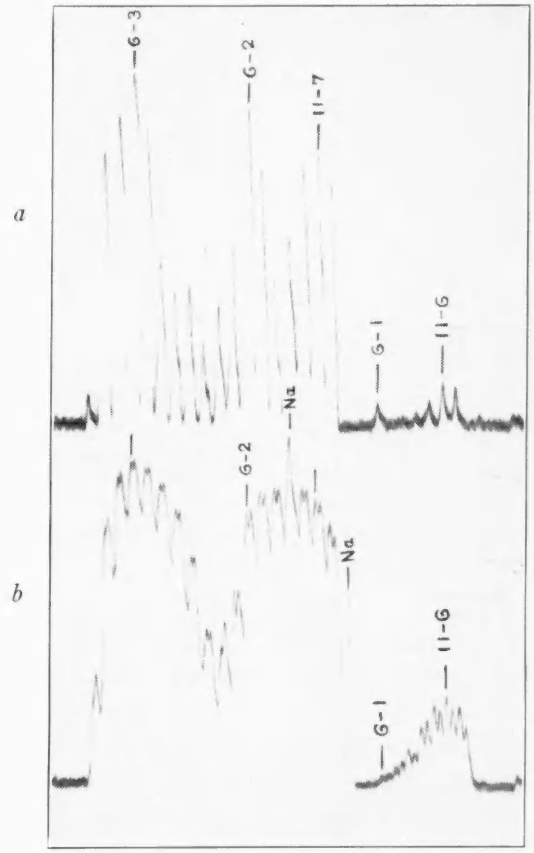

MICROPHOTOMETER CURVES OF THE FIRST POSITIVE BANDS

a) $-190°$ C, 0.2 mm *Hg*, 0.5 milliamp/cm²

b) 650° C, 0.2 mm *Hg*, 0.5 milliamp/cm²

system, in the case where the density of the exciting current is smaller, it was clearly observed that bands with smaller vibrational quantum numbers v' appear more enhanced in comparison with those with the higher v', but the effect is small in the case of the higher current density. For example, in the group $\Delta v = -3$, the band at 4059 (0,3) is much more intense than that at 3998 (1,4) when the current density is small, in spite of the fact that the intensities of both bands are nearly comparable when the current density is high. In the group $\Delta v = -4$, the bands at 4344 (0,4), 4269 (1,5), and 4201 (2,6) come into view with nearly the same intensity under the excitation of the higher current density, while the two former bands are more distinctly emitted than the latter one in a weak current excitation. In the group 4574 (1,6), 4490 (2,7), and 4416 (3,8), due to the transitions $\Delta v = -5$, the latter band is the most intense, while the first is the weakest under the excitation of a high current density, but the order is completely reversed with a low current density. In the group $\Delta v = -6$, the maximum at the band 4648 (4,10) is displaced to the band 4814 (2,8) when the exciting current density is decreased. In the negative bands, it was confirmed that similar enhancements are observable in the case of a small density of the exciting current, but, similarly to that in the case of temperature variation, the effect is not so great as that in the first and the second positive bands.

Lastly, the modifications of intensity distribution of the band system due to the variation of pressure were studied, and the conclusion was arrived at that the above-mentioned modifications of intensity distribution due to the change of temperature or of the density of the exciting current are observable in all ranges of pressure between a few mm and 0.01 mm. In the case of a very low pressure, i.e., when the velocities of the impacting electrons are relatively high, the bands from the initial levels with the higher vibrational quantum numbers are relatively enhanced in the three band systems here investigated, as G. Herzberg[4] has already confirmed, and the maximum in the band group tends to be displaced toward the band with greater v'.

It may be remarked here that the intensity modifications of the

[4] *Loc. cit.*

bands are not affected by the introduction of a considerable percentage of oxygen or of air, nor by the shape and the dimensions of the tube. Further, they do not depend to any great extent on the relative intensity of the band system as a whole. For instance, in the case where a very weak current is passed through nitrogen or through air contained in a large bulb 25 cm in diameter at pressure 0.01 mm *Hg*, the first positive and the negative bands are emitted intensely and the second positive bands are weak, while, in the case where the exciting current is weak at comparatively high pressure, the first as well as the second positive bands appear intense and the negative bands are emitted very weakly; but it was confirmed that the selective enhancements of the bands above described are observable so long as the exciting current density is small, in spite of the marked difference in the relative intensities of the three band systems. Goldstein[5] has already reported that the color of glowing nitrogen in the positive column of a Geissler tube, when immersed in liquid air, changes to golden or greenish yellow. This phenomenon is observable, however, only in the case where the gas is excited at relatively high pressure (a few mm or greater) with a comparatively high current density, while in the case of a lower current density it changes from a pink to a whitish purple or from a pink to a reddish orange, according as the pressure of the gas is high (few mm) or low (0.1 mm or less). It is also noticed that, when the discharge tube of a small section (1 cm^2) was used, the color of the glow changes to a faint blue independently of the pressure. It was confirmed that, so long as the discharging current is small, the sharp selections of the bands are always observable in the positive column, as well as in the negative glow, independently of their colors.

DISCUSSION

From the results obtained in this experiment, it is shown that the better defined and sharper the selective enhancements of the bands having the vibrational quantum numbers $v' = \sim 6$ and $v' = \sim 11$ in the first positive bands, and having $v' = \sim 0,1$ in the second positive as well as in the negative bands, are observed, the lower the temperature of the gas, and the smaller the density of the exciting current. It is also shown that this effect is observable conspicuously in the

[5] *Physikalische Zeitschrift*, **6**, 14, 1905.

first and the second positive bands and weakly in the negative bands.

It is very difficult to believe that the selective enhancements of the first positive bands are due to collisions of the second kind between the metastable molecules ($A^3\Sigma^{(o)}$) and metastable atoms (^2P and ^2D). Obviously, the probability of producing the metastable atom in the ^2D or in the ^2P state as the result of a single collision between a normal molecule and a relatively low-speed electron will be very small in comparison with the effect by which the molecule is excited or ionized, and it is reasonable to consider that the metastable atoms, if they exist, will be produced from the dissociations of the excited or ionized molecules as a result of their collisions with other molecules, or of other effects, during their life, and that their concentrations will be extremely small. Even though it is assumed that these metastable atoms exist in some concentration in the gas, the probability of their exciting the non-vibrating metastable molecules to the $B^3\Pi$ levels with special values of vibrational quantum numbers will be extremely small as compared with that of their being directly excited to these levels by the collisions between the molecules and the electrons. Therefore, it is very difficult to accept the explanation that the selective enhancements of the bands above described are due to collisions of the second kind between the metastable molecules and the metastable atoms, and it is as difficult to account for the enhancements as being due to the interaction between the upper $B^3\Pi$, or the lower $A^3\Sigma$, state and another repulsive level (predissociation), though the single-headedness and weak appearance of the band with v' greater than 13 may perhaps be explained by the theory of Kaplan.[6]

It seems that this selective enhancement of the bands will be followed quite reasonably by the assumption that the Franck-Condon principle also holds good in the case where the molecule is excited by electron impact. The approximate potential energies in the molecular states $B^3\Pi$ and $A^3\Sigma$, which are the upper and lower states for the emission of the first positive bands, are calculated by the ordinary method with the molecular constants obtained from the vibrational and rotational analysis,[7] or simply by Morse's function,

[6] *Physical Review*, **37**, 1406, 1931.

[7] S. M. Naudé, *Proceedings of the Royal Society*, **136**, 114, 1932.

and are plotted in the accompanying figure (Fig. 1). Let us assume that in the actual molecule the repulsive branch of the potential curve in the upper $B^3\Pi$ state is slightly displaced toward the greater nuclear distance in comparison with the result of approximate calculation, as shown in the broken line in the figure (or better, that the repulsive potential curve in the lower $A^3\Sigma$ state is slightly displaced toward the smaller nuclear distance). As clearly shown by the figure, the non-vibrating normal molecule will be excited directly to the $B^3\Pi^{(\sim 6)}$ or the $A^3\Sigma^{(\sim 8,7)}$ states by the electron impact, and the metastable molecule in the $A^3\Sigma^{(\sim 8,7,\ldots)}$ states may again be excited by the second impact of the electron at its near- or far-nuclear turning point of vibration to the $B^3\Pi^{(\sim 6)}$ or $B^3\Pi^{(\sim 11)}$ state, respectively, during its lifetime; therefore, the probability of producing the $B^3\Pi^{(\sim 6)}$ state is greater than that of producing the $B^3\Pi^{(\sim 11)}$ state. Thus the reason why the bands emitted by the transitions from the $B^3\Pi^{(\sim 6)}$ and the $B^3\Pi^{(\sim 11)}$ states are selectively enhanced will be understood, and the same reasoning will also apply as an explanation of the fact that the bands with $v' = \sim 6$ appear more intense than those with $v' = \sim 11$.

At lower temperatures there will be a predominance of the non-vibrating normal molecules, and the selections above described will appear very sharply defined. But as the rise in temperature of the gas causes an increase in the number of molecules in the levels with greater vibrational quantum numbers, it may be expected that the selective excitations of the levels will be small at a high temperature. The fact that the increase of the exciting current density gives rise to diffuseness in the selection of the bands can be accounted for by (1) the rise of temperature, (2) the increase in the probability of producing the $B^3\Pi$ state by the downward transitions from the higher levels, which is caused by the upward transitions from the excited states, owing to electron impact, and (3) the increase in the probability of exciting the normal molecules, while preserving their vibration, just after they have returned from the upper states. It will also be readily understood why the bands with $v' = \sim 2$ are selectively enhanced under the excitation conditions of a very weak current at low temperature, as in this circumstance some little concentration of the $A^3\Sigma$ molecules with small v'' or $v'' = 0$ will result.

The nuclear distances in the equilibrium position of nuclei in the

$C^3\Pi$ state of N_2 and in the $A'^2\Sigma$ state of N_2^+, which are the upper states of emission of the second positive and the negative bands, are 1.14 A and 1.07 A, respectively, which are not far from the corresponding value 1.09 A of the molecule in the normal state $X^1\Sigma$. Therefore, it may be reasonable to infer that, in the case where the gas is excited at a low temperature and with a very weak current, the selective enhancements of the bands with smaller vibrational

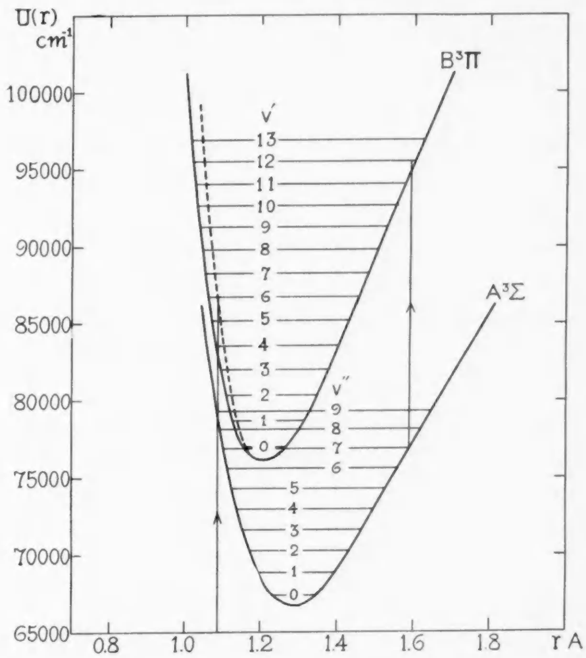

FIG. 1.—Approximate potential energy-curves for $A^3\Sigma$ and $B^3\Pi$ of N_2

quantum numbers ($v' = \sim 0,1$) are observed, while in the case of excitation at high temperature and with a greater current the excitation of the higher vibrational levels is brought about and the sharpness or distinctness of the selection is small.

As the frequencies of nuclear vibration in the $A'^2\Sigma$ state of the N_2^+ molecule are comparatively great, in spite of the fact that its dissociation energy is small, or, in other words, that the potential curve is flat and shallow; it can be inferred that the vibrational levels of the $A'^2\Sigma$ state are not so different, even though they have been excited from various different vibrational levels in the normal molec-

ular state $X^1\Sigma$ of N_2. This is the reason why the rise of temperature and the increase in the density of the exciting current have less influence on the selective enhancement in the negative bands compared with the selective enhancement in the first and the second positive bands.

As above described, the selective enhancement of the bands with special value of v', and the sharpness of selection, seem to follow as a reasonable consequence of the Franck-Condon principle when we also take into consideration the potential curves in the initial and final states of the emission. In the discussion above it was considered that the distributions of the molecules in the vibrational levels of the initial states of emission are mainly to be ascribed to the upward transitions due to collisions between the electrons and the nitrogen molecules in the normal as well as in the metastable $A^3\Sigma$ state. But in an actual case these initial states may also be caused by downward transitions from the higher energy states, and the smaller the selective enhancements of the bands may be observed, the more frequently these downward transitions from the higher levels take place.[8]

With respect to the pressure, the temperature, and the current density of excitation, the above experimental conditions resemble in some degree the conditions of the aurora as they appear in the upper atmosphere, and it will be very interesting to give some consideration to the auroral spectrum. In the aurora, it has been observed that the negative and the second positive bands appear intense, and the bands appearing have been identified as the (0,0), (0,1), (0,2), (1,2), (1,3), and (2,3) bands among the negative bands, and also the (0,0), (0,1), (0,2), (0,3), (0,4), (1,0), (1,2), (1,3), (1,4), (1,5), (2,1), (2,3), (2,4), (2,5), (3,3), and (3,4) bands among the second positive bands, while the bands at 6465, 5945, 6320 and 6565 A have also been identified as (8,5), (8,4), (10,7), and (7,4?) among the first positive bands.[9] Recently L. Vegard[10] has reported that he has found two bands in the auroral spectrum in the infrared region, a strong one at 7883 and a weak one at 8095 A. These bands were found to have sharp edges toward the longer wave-

[8] Herzberg, *loc. cit.*

[9] J. C. McLennan, *Proceedings of the Royal Society*, **120**, 327, 1928.

[10] *Nature*, **129**, 468, 1932.

lengths. Taking into consideration the great intensity of these two bands and the emission of the second positive bands of nitrogen in the auroral spectrum, he has interpreted them as the appearance of the first positive bands of nitrogen with a special distribution of intensity. These two bands may probably be identified with the bands 7896 (7,6) and 8047 (6,5) in the first positive bands, in accordance with Vegard's view, and also as a result of the above experiments, though, in the latter band, some difference in the wavelength is found.

From the above results, it seems that in the negative as well as in the second positive bands, those emitted by the transition from the initial levels with small quantum numbers v', are quite similarly enhanced both in the aurora and in this arrangement of experiments, as far as the exciting current density is small and the temperature of the gas is low. In the first positive bands, those with $v'=7$ or 8 and ~ 10 are specially enhanced in aurorae, instead of those with 6 or 7 and ~ 11 in the experiment, and no enhancements of the bands with the vibrational quantum number $v'=\sim 2$ in the aurora were found in disagreement with the experimental results.

McLennan[11] has already attempted to explain the rare occurrence of the forbidden lines (nebular lines or auroral green line) in terrestrial sources by the fact that the collisions of the second kind between the excited atoms and other atoms, or between the former and the surfaces of a discharge tube, are frequently taking place. Similarly, it will be inferred that, in the experimental conditions, the metastable $A^3\Sigma$ molecules in any vibrational quantum state collide frequently with other molecules, or with the surfaces of a discharge tube, and, therefore, that they are not only capable of being excited from the levels with $v''=\sim 8$ or 7, but also from the levels with smaller v'' or with $v''=0$, one part of which is produced by the loss of vibrational energy due to the collisions above mentioned, during their lifetime. Hence, the reason why the first positive bands with $v'=\sim 2$ or with v' thereabouts appear more enhanced in the experimental conditions than in the aurora will be understood.

In the case where the normal molecules of nitrogen are excited by low-speed electrons, the greatest predominance of the excited molecules in the vibrational levels with $v'=\sim 6$ in the upper B state will

[11] *Loc. cit.*

result, but in the case of excitation with high-speed electrons, they will be excited to higher vibrational levels than those with $v' = \sim 6$ in that state. Therefore, if it is assumed that a great number of the electrons exciting the auroral spectrum have higher velocities than those in the discharge tube used in this experiment, it will be reasonably conceivable that in the aurora the intensity maximum in the band group displaces toward the band with the higher quantum number v' compared with that in the band group observed in the experiments. The enhanced appearance of the negative bands in the aurora seems to suggest that there are some concentrations of high-speed electrons in it, and this fact serves to give favorable support to the above consideration.

The displacement of the intensity maximum may also be explained in the same manner as Lord Rayleigh[12] and also McLennan[13] have already suggested in their consideration of the intensity distribution of the α bands of active nitrogen, in the case where a suitable quantity of inert gas is mixed with nitrogen. If the $A^3\Sigma$ molecules are excited by electron impact, after their vibrational levels have descended to $v'' = 7, 6, 5, \ldots$ from $v'' = 8$ or 7 in consequence of collisions with other molecules or atoms during their lifetime, it is to be expected that there result the $B^3\Pi$ molecules with $v' = 10, 9, 8, \ldots$, and this result causes the displacement of the intensity maximum in the band group in the observed direction, as shown in the results of observation.

Or, it might be better to consider the displacements as due partly to the first possibility, and the other to the second possibility, i.e., to consider that the displacement of the intensity maximum at the band with $v' = \sim 6$ toward the band with $v' = 7$ or 8 is to be attributed to the first possibility, while the displacement of the maximum at the band with $v' = \sim 11$ toward the band with $v' = \sim 10$ is to be attributed to the second.

PHYSICAL LABORATORY
SENDAI, JAPAN
July 1932

[12] *Proceedings of the Royal Society*, **102**, 453, 1923.
[13] *Loc. cit.*

A STATISTICAL STUDY OF THE ROTATIONAL BROADENING OF STELLAR ABSORPTION LINES IN CLASSES B AND O

By CHRISTINE WESTGATE

ABSTRACT

The axial rotation of stars, as determined by the broadening of the *Mg* II line λ 4481, and of the *He* I line λ 4472, is studied statistically for 275 stars of class B. The widths of these lines in Angstrom units were transformed into their corresponding equatorial velocities in kilometers per second. The observed frequency graph is compared with a theoretical curve which was constructed with regard to the probability of different inclinations of axes and with the assumption of an arbitrary distribution of equatorial velocities among stars. The best approximation to the observed curve is obtained by assuming that 27 per cent of the stars have $V_0 = 50$ km per second; 53 per cent, $V_0 = 100$; 15 per cent, $V_0 = 150$; 4 per cent, $V_0 = 200$; and 1 per cent, $V_0 = 250$.

1. The purpose of this paper is to give a list of the widths of the two absorption lines *Mg* II λ 4481 and *He* I λ 4472 for the brighter B-type stars, and then to investigate the distribution of real equatorial velocities. In the last section we shall assume that the broadening of these lines is caused by the Doppler effect of axial rotation.

2. Single-prism spectrograms which had been taken with the Bruce spectrograph attached to the Yerkes 40-inch refractor were available for more than 275 stars of apparent magnitude brighter than about 5.5. The linear dispersion is 30 A per millimeter at λ4500.

Whenever possible, the widths of λ 4481 and of λ 4472 were measured under a comparator on two plates of each star. In the case of λ 4481, Δλ was measured on two plates for 136 stars, with an average difference of 0.2 A. The average difference of the width of λ 4472 for 196 stars is slightly less than 0.3 A. The adopted widths of the two lines are contained in columns 2 and 3 of Table I.

3. In Figure 1 my measurements are compared with the measurements published by O. Struve[1] for the widths of these two absorption lines in 46 spectroscopic binaries of class B. Although the scatter is large, the majority of the points lie within a 45° belt, indicating a one-to-one correlation. The scatter is due primarily to the difficulty of accurately and consistently setting a cross-hair on the apparent edge of an absorption line.

[1] *Monthly Notices of the Royal Astronomical Society*, **89**, 231, 1929.

TABLE I

Boss Number	Average Width λ 4481	Average Width λ 4472	Rotational Velocities in Km/Sec. Derived From λ 4481	Rotational Velocities in Km/Sec. Derived From λ 4472	Adopted V
5	2.3	....	100	....	100
27	0.8	1.0	0	0	0
68	2.1	....	90	....	90
103	....	2.0	....	50	50
118	1.1	1.5	0	30	10
122	1.0	1.1	0	10	10
123	1.3	0.9	40	0	20
141	....	2.0	....	50	50
149	....	2.6	....	80	80
159	1.1	0.5	0	0	0
201	1.0	....	0	....	0
212	1.1	0.9	0	0	0
224	1.0	....	0	....	0
257	1.3	1.5	40	30	30
263	1.3	0.5	40	0	20
265	1.6	1.2	60	20	50
379	1.5	....	60	....	60
412	....	2.9	....	90	90
419	1.2	1.4	20	20	20
425	1.1	1.4	0	20	10
459	2.2	1.8	100	40	80
620	2.5	1.9	110	40	80
627	1.3	0.8	40	0	20
641	1.6	1.9	60	40	50
708	1.5	1.9	60	40	50
740	2.5	2.8	110	80	100
742	2.0	3.5	90	120	110
761	1.2	1.5	20	30	20
767	....	4.2	....	140	140
780	1.8	2.7	80	80	80
781	1.5	1.5	60	30	40
790	4.5	2.9	200	90	140
802	1.7	....	70	....	70
806	2.6	....	120	....	120
816	1.1	....	0	....	0
837	1.8	3.0	80	90	80
839	1.5	1.7	60	40	40
852	2.9	2.9	130	90	110
856	2.3	2.4	100	70	90
857	3.0	....	130	....	130
860	1.1	1.1	0	10	10
863	1.5	3.3	60	110	80
874	1.5	2.7	60	80	70
893	3.2	2.5	140	70	120
894	1.6	2.4	60	70	70
896	1.7	2.0	70	50	60
898	....	3.5	....	120	120
902	1.0	1.8	0	40	20
904	....	3.7	....	120	120
910	....	3.0	....	90	90
913	....	3.1	....	100	100

TABLE I—*Continued*

Boss Number	Average Width		Rotational Velocities in Km/Sec. Derived From		Adopted V
	λ 4481	λ 4472	λ 4481	λ 4472	
920	....	3.0	....	90	90
926	1.1	3.9	90	130	110
934	1.9	2.5	80	70	80
947	....	2.3	....	60	60
956	1.1	2.0	0	50	20
981	1.8	1.9	80	40	60
992	....	0.9	....	0	0
997	0.9	....	0	....	0
1003	1.0	1.7	0	40	20
1039	4.1	4.2	180	140	160
1079	1.3	1.5	40	30	30
1107	1.8	3.1	80	100	90
1123	....	4.1	....	140	140
1139	....	2.4	....	70	70
1147	1.3	1.4	40	20	30
1159	....	1.7	....	40	40
1192	1.0	2.0	0	50	20
1203	1.6	....	60	....	60
1204	2.9	3.4	130	110	120
1213	1.0	....	0	....	0
1216	2.1	2.9	90	90	90
1242	2.2	1.8	100	40	80
1249	....	1.1	....	10	10
1250	1.5	1.3	50	20	40
1262	1.7	2.1	70	50	60
1274	2.0	2.3	90	60	70
1277	....	2.2	....	60	60
1284	1.0	1.3	0	20	10
1297	1.3	2.3	30	60	50
1301	....	1.9	....	40	40
1303	1.7	2.3	70	60	70
1304	1.5	1.5	60	30	40
1313	....	2.1	....	50	50
1314	....	3.0	....	90	90
1315	1.8	2.0	80	50	60
1332	....	2.1	....	50	50
1333	2.0	2.3	90	60	80
1336	1.7	2.2	70	60	60
1339	....	3.5	....	120	120
1340	2.2	2.1	100	50	70
1343	....	1.9	....	40	40
1346	....	4.0	....	140	140
1353	0.9	2.0	0	50	20
1354	....	2.7	....	80	80
1357	....	2.1	....	50	50
1361	....	2.2	....	60	60
1362	1.4	1.9	50	40	50
1363	....	1.3	....	20	20
1364	....	2.7	....	80	80
1365	....	2.9	....	90	90
1366	....	2.7	....	80	80

TABLE I—*Continued*

Boss Number	Average Width		Rotational Velocities in Km/Sec. Derived From		Adopted V
	λ 4481	λ 4472	λ 4481	λ 4472	
Bond 640	....	3.2	....	100	100
Bond 619	....	2.9	....	90	90
Bond 708	....	1.9	....	40	40
1370	....	1.8	....	40	40
1388	1.9	1.5	80	30	50
1389	....	2.5	....	70	70
1391	....	3.9	....	130	130
1396	....	2.6	....	80	80
1398	....	3.4	....	110	110
1399	....	2.0	....	50	50
1428	1.7	2.5	70	70	70
1435	....	2.0	....	50	50
1438	1.1	....	0	....	0
1454	....	3.7	....	120	120
1464	....	2.6	....	80	80
1475	....	2.9	....	90	90
1504	1.0	1.4	0	20	20
1507	2.3	1.8	100	40	60
1523	1.2	1.3	20	20	20
1525	....	2.1	....	50	50
1548	....	3.1	....	100	100
1550	....	4.4	....	150	150
1554	1.1	1.8	0	40	20
1568	1.6	2.8	60	80	70
1572	1.4	....	50	....	50
1594	2.3	2.8	100	80	90
1598	....	2.5	....	70	70
1601	1.8	1.2	80	20	50
1603	....	3.5	....	120	120
1609	1.5	2.1	60	50	50
1634	....	3.0	....	90	90
1639	....	5.8	....	210	210
1640	....	3.7	....	120	120
1640	....	3.9	....	130	130
1660	1.8	1.9	80	40	60
1686	1.8	....	80	....	80
1706	....	1.9	....	40	40
1730	....	1.8	....	40	40
1744	....	2.4	....	70	70
1754	2.3	2.8	100	80	90
1781	....	1.9	....	40	40
1793	1.6	2.0	60	50	60
1804	2.2	2.2	100	60	80
1812	....	4.7	....	170	170
1817	1.6	2.3	60	60	60
1819	1.4	....	50	....	50
1872	....	2.8	....	80	80
1877	1.6	3.1	60	100	80
1899	....	1.8	....	40	40
1901	....	2.5	....	70	70
1924	1.7	1.8	70	40	60

TABLE I—*Continued*

Boss Number	Average Width		Rotational Velocities in Km/Sec. Derived From		Adopted V
	λ 4481	λ 4472	λ 4481	λ 4472	
2071	1.5	....	60	....	60
2158	....	3.3	....	110	110
2330	2.0	3.1	90	100	90
2342	1.0	1.5	0	30	10
2365	1.1	....	0	....	0
2445	1.1	1.2	0	20	10
2451	2.5	....	110	....	110
2465	1.0	....	0	....	0
2492	1.9	....	80	....	80
2600	....	3.9	....	130	130
2690	1.9	....	80	....	80
2698	4.7	4.2	210	140	190
2788	3.2	....	140	....	140
2792	2.1	2.5	90	70	80
2804	....	2.8	....	80	80
3045	2.1	3.5	90	120	110
3138	....	3.0	....	90	90
3191	1.3	....	40	....	40
3392	2.7	....	120	....	120
3476	3.5	3.9	160	130	140
3566	3.2	4.0	140	140	140
3653	1.6	....	60	....	60
3767	1.8	....	80	....	80
3944	....	4.6	....	160	160
3955	1.1	1.6	0	30	20
3973	....	3.5	....	120	120
4008	1.8	2.8	80	80	.80
4062	....	2.3	....	60	60
4066	....	3.7	....	120	120
4086	....	2.7	....	80	80
4089	1.2	....	20	....	20
4093	....	3.1	....	100	100
4112	1.2	....	20	....	20
4117	....	3.2	....	100	100
4162	1.5	1.6	60	30	40
4183	....	3.1	....	100	100
4218	1.4	1.6	50	30	40
4302	3.5	....	160	....	160
4368	1.6	1.8	60	40	50
4388	....	2.8	....	80	80
4399	1.8	2.0	80	50	60
4465	2.8	2.7	120	80	100
4479	1.3	1.7	40	40	40
4548	1.4	1.6	50	30	40
4562	1.4	2.1	50	50	50
4590	1.9	2.3	80	60	70
4604	2.3	2.1	100	50	90
4620	1.6	2.0	60	50	60
4702	1.5	....	60	....	60
4721	1.6	....	60	....	60
4739	1.7	....	70	....	70

TABLE I—*Continued*

Boss Number	Average Width		Rotational Velocities in Km/Sec. Derived From		Adopted V
	λ 4481	λ 4472	λ 4481	λ 4472	
4779	1.1	....	0	....	0
4783	1.5	1.9	60	40	50
4784	....	4.2	....	140	140
4794	....	2.6	....	80	80
4816	2.0	....	90	....	90
4842	1.2	2.7	20	80	40
4864	2.2	2.2	100	60	90
4883	....	4.3	....	150	150
4897	1.5	1.7	50	40	50
4906	1.7	2.5	70	70	70
4917	....	4.6	....	160	160
4934	1.8	2.0	80	50	60
4942	1.5	1.8	60	40	50
4949	....	2.8	....	80	80
4992	1.1	1.5	0	30	10
5004	1.8	2.7	80	80	80
5018	....	2.8	....	80	80
5024	1.3	....	40	....	40
5068	....	5.1	....	180	180
5097	1.7	4.0	70	140	90
5102	1.5	2.6	60	80	70
5127	....	4.0	....	140	140
5156	....	3.6	....	120	120
5170	....	5.2	....	190	190
5190	....	3.2	....	100	100
5240	2.2	....	100	....	100
5265	....	3.5	....	120	120
5272	1.8	1.9	80	40	60
5298	1.4	2.3	50	60	60
5310	2.6	2.4	120	70	100
5325	1.4	1.9	50	40	50
5350	2.2	2.6	100	80	90
5361	2.1	1.9	90	40	80
5366	1.5	....	60	....	60
5375	1.4	2.1	50	50	50
5453	1.6	1.9	60	40	50
5465	1.9	....	80	....	80
5471	....	3.6	....	120	120
5516	1.6	2.6	60	80	70
5525	....	4.7	....	170	170
5563	2.0	2.0	90	50	70
5580	1.3	2.2	40	60	50
5609	2.0	1.8	90	40	60
5627	....	3.2	....	100	100
5639	1.4	1.6	50	30	40
5680	3.7	....	160	....	160
5687	....	2.3	....	60	60
5706	0.9	1.2	0	20	0
5719	....	3.4	....	110	110
5755	1.3	1.7	40	40	40
5757	1.4	2.3	50	60	60

TABLE I—*Continued*

Boss Number	Average Width		Rotational Velocities in Km/Sec. Derived From		Adopted V
	λ 4481	λ 4472	λ 4481	λ 4472	
5763	2.5	2.8	110	80	100
5764	1.6	1.4	60	20	40
5777	....	3.2	....	100	100
5779	1.2	1.7	20	40	30
5810	....	2.2	....	60	60
5833	....	3.9	....	130	130
5844	1.2	1.6	20	30	30
5853	3.7	3.9	160	130	150
5856	3.0	2.1	130	50	80
5913	....	2.3	....	60	60
5918	....	5.7	....	210	210
5955	1.8	1.9	80	40	60
5992	....	4.1	....	140	140
6009	3.2	3.2	140	100	120
6046	2.3	3.0	100	90	100
6073	2.0	2.4	90	70	80
6075	2.4	....	110	....	110
6095	3.6	....	160	....	160
6155	....	2.5	....	70	70
6169	2.6	....	120	....	120

In Figure 2 my observations of the widths of *Mg* II λ 4481 (*a*) and of *He* I λ 4472 (*b*) are plotted against the rotational velocities determined by C. T. Elvey for 25 of the same stars.[2]

The observed stars, whose spectral types were taken from the *Henry Draper Catalogue*, are distributed in spectral class as follows: O, 12; B0, 14; B1, 15; B2, 24; B3, 90; B5, 44; B8, 49; B9, 27. Table II gives for each class the average width of each line and in parentheses the number of stars used in obtaining that average. There is a slight increase in the width of *He* I λ 4472 for classes B2 and B3, corresponding to the maximum of intensity of this line. For *Mg* II λ 4481 there is no measurable change in Δλ with spectral type.

4. Since it is more desirable to work with the observed rotational velocities themselves, I have converted my line widths into velocities by means of the curves in Figure 2. The curve for λ 4481 is probably more reliable and fits the observations by Elvey reasonably well. It indicates that a line width of about 1.1 A corresponds to zero rotational velocity, and that for very wide lines the rotational velocity is

[2] *Astrophysical Journal*, **71**, 221, 1930.

proportional to $\Delta\lambda$.[3] The curve for λ 4472 is very uncertain. I have adopted one of the two regression lines (*A* in Fig. 2*b*) of the scatter diagram (for which Pearson's coefficient of correlation is 61 per cent). There are not enough stars in common with Elvey to justify this choice, and the scatter is disappointingly large, but it seemed to be better to use this graphical conversion than the mere assumption that $\Delta\lambda$ is equivalent to the equatorial velocity of rotation. The results derived for λ 4481 and for λ 4472 are in fair agreement with one another. The average difference for each star is about 25 km per second. The

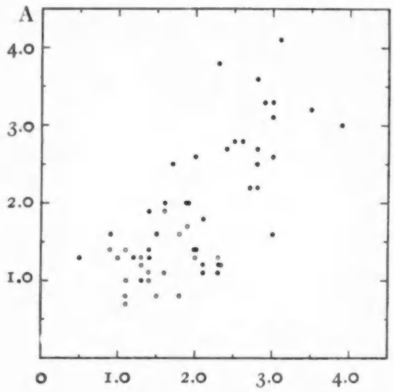

FIG. 1.—Width, in angstroms, of λ 4472 (dots) and λ 4481 (circles). Abscissae: author's measures; ordinates: Struve's measures for same stars.

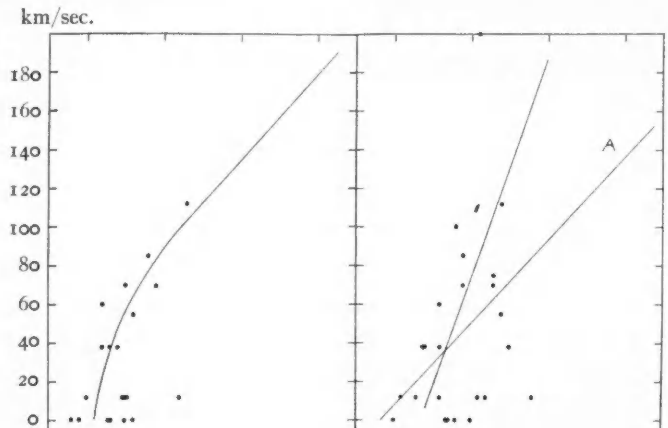

FIG. 2.—Comparison of Elvey's determinations of rotational velocities with author's measurements of widths of λ 4481 (*a*), and of λ 4472 (*b*) for same stars.

[3] By assuming that zero rotational velocity corresponds to $\Delta\lambda = 1.1$ A, we make allowance for abundance broadening. This eliminates almost completely the question of finite resolving power of the spectrograph, since for the Yerkes instrument the width of a monochromatic line would be measured as approximately 0.6 A.

observed rotational velocities obtained by this means from measurements of each of the two lines are contained in columns 4 and 5 of Table I, and the weighted mean of these two velocities is given in column 6.

TABLE II

	λ 4472	λ 4481		λ 4472	λ 4481
O	(12) 2.4		B3	(89) 2.7	(43) 1.7
Bo	(14) 2.5		B5	(41) 2.4	(38) 1.8
B1	(15) 2.3	(7) 1.8	B8	(26) 2.0	(49) 2.0
B2	(24) 2.7	(11) 1.9	B9	(8) 1.9	(26) 1.6

5. The observed frequencies of different widths of λ 4481 and of λ 4472 are given in Figure 3. In (*a*) the continuous line gives for λ 4481 the number of stars in ranges of 1 A and the dotted line in ranges of 0.5 A. Part (*b*) gives the frequencies of line widths of

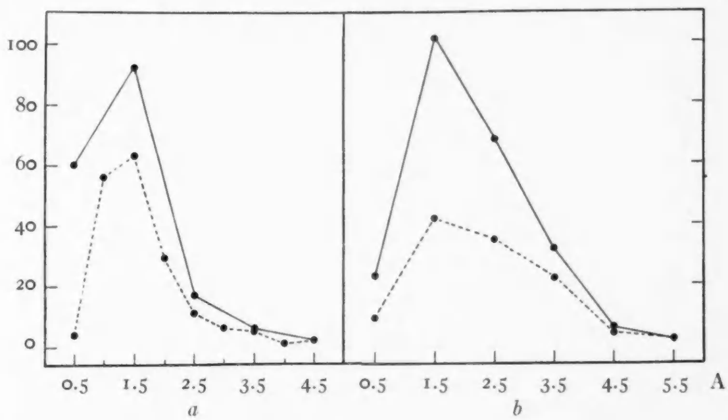

FIG. 3.—Ordinates are numbers of stars. (*a*) Continuous line is for ranges of line width of 1 A (0.5–1.5 A, etc.); dotted line for 0.5 A (0.5–1.0 A, etc.). (*b*) Continuous line includes all stars and dotted line only those of subdivisions B2 and B3.

λ 4472. The smooth line gives the data from all stars and the dotted line gives the data from subdivisions B2 and B3 alone. The choice of a smaller range of Δλ seems to have no effect upon the general shape of the frequency-curve for λ 4481. The maximum frequency for both λ 4481 and λ 4472 occurs at a line width of from 1.5 to 2.5 A.

The continuous line in Figure 4 gives the number of stars having observed velocities of 0–50, 50–100, 100–150 km per second, etc. These velocities are, of course, the projection upon the line of sight of the true equatorial velocities of rotation, $V_0 \sin i$, where V_0 is the equatorial rotational velocity and i is the inclination of the axis of

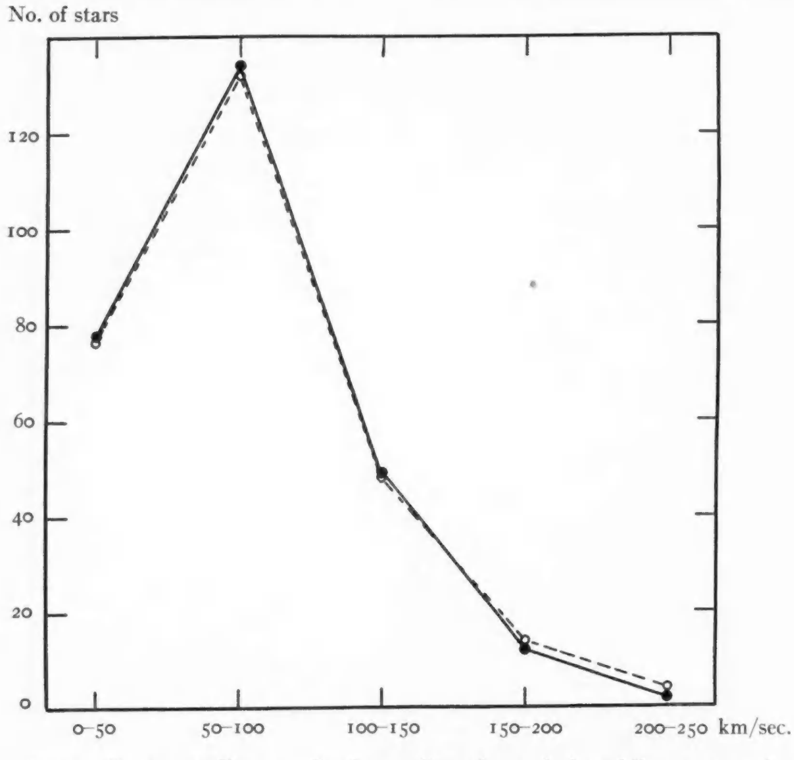

FIG. 4.—Frequency diagram. Continuous line, observed; dotted line, computed.

the star to the line of sight. For the problem of determining the distribution of real rotational velocities we assume that the directions of the axes of rotation are distributed at random for all the stars in the sky. Suppose, for a moment, that all stars have the same equatorial rotational velocity, V_0. In that case the number of stars which would have an inclination between i_1 and i_2, and consequently would have velocities between $V_0 \sin i_1$ and $V_0 \sin i_2$, will be proportional to the area of the zone of the celestial sphere described by an

axis corresponding to i_1 and an axis corresponding to i_2 as they rotate about the line of sight. Near an inclination of 0° this area will be very small and approach 0, and at 90° it will be a maximum. The area of the zone is ($\cos i_1 - \cos i_2$) of the half-sphere. These factors for the five equal divisions of $V_0 \sin i$, when multiplied by the

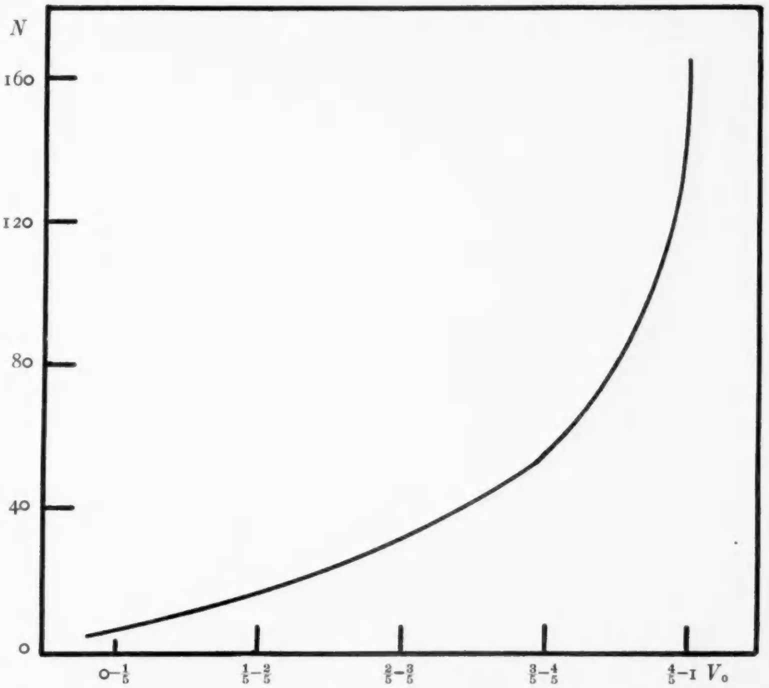

FIG. 5.—Theoretical frequency diagram for the case in which all stars have the same actual rotational velocities and observed differences are due to inclinations of axes.

total number of stars used in my observed frequency graph, give a theoretical frequency-curve for the case in which all the stars have the same V_0, and differences in observed velocities are due simply to inclination. This curve, Figure 5, has no resemblance to the original and we conclude that not all stars have an equal V_0.

I have next assumed an arbitrary frequency distribution for V_0. For any given value of V_0 we obtain a curve similar in shape to that of Figure 5. The ordinates of each curve are multiplied by factors

which are proportional to the postulated frequency of each given V_0, and the ordinates of all curves are summed to give the integrated effect for all values of V_0 and for all i's. By trial and error a distribution of frequencies for V_0 was found (Table III) which agrees almost exactly with the observed curve (see dotted line in Fig. 4).

TABLE III

V	Assumed Distribution (in Per Cent)	V	Assumed Distribution (in Per Cent)
50	27	200	4
100	53	250	1
150	15		

It is probably safe to conclude that four-fifths of the 275 B-type stars studied have rotational velocities from 0 to 100 km per second, that the number of stars with velocities of 200 km per second or greater is very small (5 per cent) and that the most frequent value of V_0, for the B stars, is around 100 km per second.

It is a pleasure to acknowledge Dr. Struve's suggestion of the problem and of the method by which it might be carried out.

YERKES OBSERVATORY
November 1932

NOTES

RAYLEIGH SCATTERING IN INTERSTELLAR SPACE

ABSTRACT

A computation of the apparent brightness of the sky was made under the assumption that the observed reddening of distant stars is caused entirely by Rayleigh scattering. The result, for solid particles, is 3.0 stellar mag. per square degree for the scattering of general starlight in galactic space, and 7.3 mag. per square degree for sunlight scattered in and near the solar system. Scattering by atoms of interstellar gas is negligible. Since the total observed brightness of the night sky is 4.5 mag. per square degree, the density of the scattering particles is probably somewhat smaller than that obtained from the effect of reddening of distant stars.

Recent investigations by R. J. Trumpler,[1] C. Schalén,[2] C. T. Elvey,[3] J. Stebbins,[4] E. T. R. Williams,[5] and others have shown rather convincingly that distant stars are redder than near ones. W. Gleissberg[6] has investigated all available observational data, and has derived, with the help of formulae by E. Schoenberg,[7] the approximate number of particles per unit volume, N, needed to produce the observed amount of reddening by Rayleigh scattering. The coefficient of scattering depends upon the refractive index of the medium, and consequently N is also a function of the refractive index. For atoms of air, $N_1 = 1.3 \times 10^4$ per cubic centimeter. For solid particles, Gleissberg finds $10^{-3} < N_2 < 10^{-2}$ per cubic centimeter. We shall assume here that $N_2 = 5 \times 10^{-3}$ per cubic centimeter. The value of N_1 is inconsistent with the results[8] I obtained from the intensities of the interstellar calcium lines, which gave $N_1 = 10^{-2}$ per cubic centimeter. Consequently, it is more plausible that scattering is produced by solid particles (or by free electrons).

If the reddening of distant stars is actually caused by Rayleigh

[1] *Lick Observatory Bulletins*, **14**, 154, 1930.

[2] *Upsala Meddelande*, **53**, 1931.

[3] *Astrophysical Journal*, **74**, 298, 1931; *ibid.*, **75**, 354, 1932.

[4] Unpublished; see *Publications of the Astronomical Society of the Pacific*, **44**, 365, 1932.

[5] *Astrophysical Journal*, **75**, 386, 1932.

[6] *Astronomische Nachrichten*, **246**, 329, 1932.

[7] *Mitteilungen der Sternwarte, Breslau*, **3**, 1932.

[8] *Monthly Notices of the Royal Astronomical Society*, **89**, 585, 1929.

scattering, then the radiation which is lost by the direct beam of light must illuminate the diffuse medium, and the color of the medium must be bluer than that of the incident light. An application of this idea to diffuse nebulae, by Struve, Elvey, and Keenan, will appear in an early issue of this *Journal.* We shall here attempt to compute the apparent brightness of the sky, under the assumption that there are 5×10^{-3} particles per cubic centimeter which scatter according to Rayleigh's law.

The formulae which I have used were derived by Charles Fabry[9] and have been adapted by me to this particular problem. There are four cases to be considered: (1) scattering of general starlight by solid particles in the galaxy; (2) scattering of sunlight by solid particles, in and near the solar system; (3) scattering of starlight by interstellar gas; and (4) scattering of sunlight by interstellar gas. We shall limit this discussion to Rayleigh scattering, leaving scattering from free electrons out of consideration. For cases 1 and 3 I have used the following equation, in which the unit of length is the meter:

$$m_0 = m + 8.8 - 2.5 \log\left[\frac{1.5h\delta}{K}\right].$$

Here m_0 is the apparent brightness of the diffuse medium, as observed from the earth, expressed in stellar magnitudes per square degree; m is the apparent magnitude of all stars together, as seen from any point of the diffuse medium. We assume that this is a constant for the whole extent of the diffuse medium, and that it is equivalent[10] to 1674 stars of $+1.0$ mag., this value being based upon the observations of Van Rhijn.[11] Accordingly, $m=-7.0$; h is the total thickness of the medium, which we assume to be 10,000 parsecs, or 3.0×10^{20} m; δ is the ratio N/N_0 where N_0 is Loschmidt's number (3×10^{19} per cubic centimeter, or 3×10^{25} per cubic meter); K is a constant depending upon the index of refraction, μ_0, of the medium under atmospheric pressure and temperature 0° C:

$$K = \frac{\lambda^4 N_0}{2\pi^2(\mu_0 - 1)^2},$$

[9] *Journal de physique,* **7,** 89, 1917.

[10] Gerasimovič and Struve, *Astrophysical Journal,* **69,** 16, 1929.

[11] *Publications of the Astronomical Laboratory, Groningen,* **31,** 37, 1921.

where λ is the wave-length for which the amount of scattered light is being computed. For λ 4500 we get:

	K
Air	0.7×10^6
Hydrogen	3.2×10^6
Solid particles	0.24

For solid particles our computation gives $m_0=+3.0$, and for a gas, $m_0=+19.2$. Cases 2 and 4 are solved by means of the equation

$$m_0=m+8.8-2.5\left[\log \delta\,\frac{D}{2K}\left(\frac{3a}{\sin a}+\cos a\right)\right],$$

where m is now the apparent photographic magnitude of the sun, -26.0; D is the mean distance earth – sun, 1.5×10^{11} m; and $(180^\circ-a)$ is the angle at the observer between the point of the sky investigated and the sun. The variation of m_0 with a has been investigated by Fabry;[12] m_0 is a minimum for $a=0$, and approaches ∞ for $a=180^\circ$. But since the latter represents the direction toward the sun, this does not concern us. For $a=90^\circ$, m_0 has a value which is 1.18 times that obtained for $a=0$. Our computation for $a=0$ gives $m_0=+7.3$ for solid particles and $m_0=+23.5$ for an interstellar gas.

It would seem that the illumination of the night sky produced by Rayleigh scattering from gas atoms is negligible. Scattering of sunlight from solid particles should be perceptible, if $N_2=5\times 10^{-3}$ per cubic centimeter. But scattering of general starlight from solid particles gives an unexpectedly large value of m_0.

Actual observations show that the brightness of the sky at night is about 4.5 mag. per square degree. Fabry[13] gives 5.0 mag., J. Dufay[14] finds 4.63 mag. for visual light and 4.37 mag. for photographic light, and Elvey[15] finds with the photo-electric photometer about 4.5 mag. per square degree. Dufay concludes from his measurements that about one-half of the illumination of the night sky is accounted for by faint stars, zodiacal light, etc., so that the unaccounted-for bright-

[12] *Op. cit.*

[13] *Comptes rendus de l'Académie des Sciences*, **150**, 272, 1910; *Astrophysical Journal*, **31**, 394, 1910.

[14] *Bulletin de l'Observatoire de Lyon*, **10**, 1928; *Journal de physique*, **10**, 219, 1929.

[15] Private communication.

ness of the sky is roughly 5.2 mag. per square degree. He states, however, that this diffuse light is not blue like the daylight sky, but is as yellow as the sun. We should therefore expect that only a small part—perhaps not more than 6.0 mag. per square degree—can possibly be left over for Rayleigh scattering in interstellar space.

There remains the possibility that our assumptions for cases 1 and 3 were incorrect. Our formula neglects general absorption of the scattered light in space, but this is probably not serious. It is much more probable that we are incorrect in assuming a constant value for m equal to that observed near the sun.[16] On the other hand, our distance, $h = 10{,}000$ parsecs, is probably underestimated, and this would tend to balance an error in m. Unless the latter is very greatly in error, we shall have to conclude that N is smaller than we have assumed. A factor of 10 in N would change m_0 by 2.5 mag. It is not unlikely that a value of $N = 5 \times 10^{-4}$ particles per cubic centimeter is still reconcilable with the observed amount of reddening. If this should not be the case, we should have to attribute at least a part of the reddening of distant stars to a cause other than Rayleigh scattering.

OTTO STRUVE

YERKES OBSERVATORY
February 2, 1933

[16] Our value, $m = -7.0$, is derived by applying a correction for atmospheric absorption to the result of Van Rhijn. His measurements gave for the total amount of starlight in both hemispheres 1440 stars of mag. 1.0 on the Harvard scale (corrected to the zenith). In a later paper Seares, Van Rhijn, Joyner, and Richmond found from star counts 1092 stars of mag. 1.0 on the International Scale (*Astrophysical Journal*, **62**, 373, 1925).